PROJECT SYNOPSIS ON

MINI IMPULSE SOLAR PLANE

Project Synopsis submitted in partial fulfillment of the degree of

BACHELOR OF ENGINEERING

BY
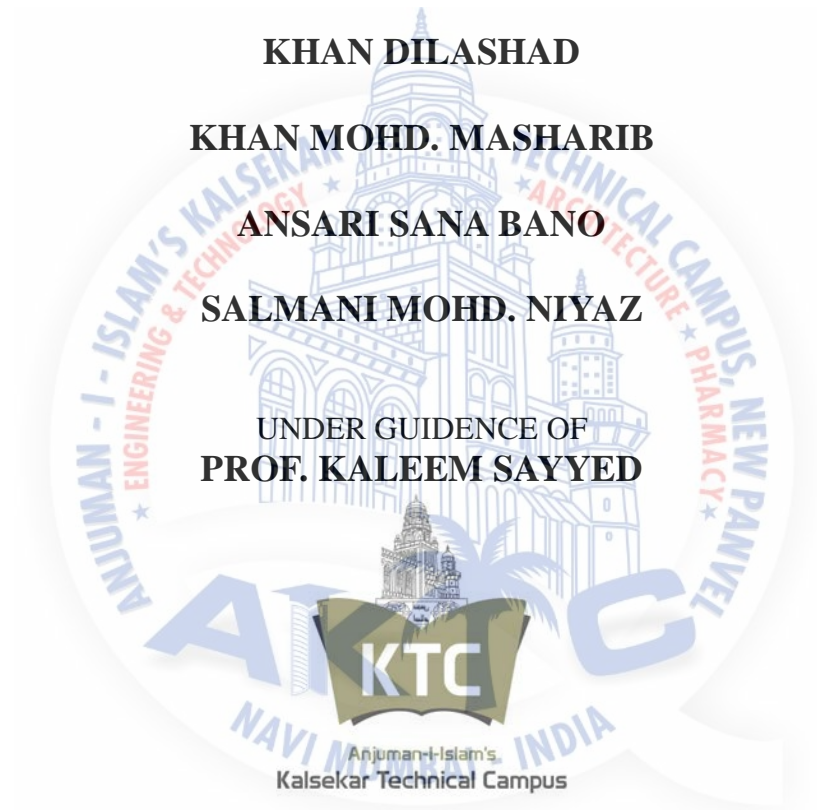
KHAN DILASHAD

KHAN MOHD. MASHARIB

ANSARI SANA BANO

SALMANI MOHD. NIYAZ

UNDER GUIDENCE OF
PROF. KALEEM SAYYED

DEPARTMENT OF ELECTRICAL ENGINEEING
AANJUMAN-I-ISLAM'S KALSEKAR TECHNICAL CAMPUS
SCHOOL OF ENGINEERING AND TECHNOLOGY
(Affiliated to University of Mumbai)
ACADEMIC YEAR 2016-17

KTC

Anjuman-I-Islam's
Kalsekar Technical Campus

SYNOPSIS OF PROJECT WORK

NAME OF THE PROJECT: - SOLAR PLANE

NAME OF THE STUDENTS & ROLL NO: -

KHAN DILSHAD	**14DEE53**
KHAN MOHD. MASHARIB	**14DEE54**
ANSARI SANA BANO	**14DEE49**
SALMANI MOHD. NIYAZ	**14DEE61**

CLASS & BRANCH: - B.E ELECTRICAL ENGINEERING

NAME OF THE COLLEGE: - ANJUMAN-I-ISLAM'S KALSEKAR TECHNICAL
CAMPUS SCHOOL OF ENGINEERING AND
TECHNOLOGY, NEW PANVEL

SEMESTER: - VII

PROJECT GUIDE   EXTERNAL EXAMINER   HEAD OF THE DEPT
PROF. SYED KALIM   PROF. SYED KALIM

ACKNOWLEDGEMENT

Among the wide panorama of people who provided us help and motivation to complete our project, we are grateful in presenting to you the rare shades of technology by documenting project "SOLAR PLANE".

We wish to express our deep sense of gratitude to our DIRECTOR DR. ABDULRAZAK HONNUTAGI for providing us the facilities to bring this project a success.

We acknowledge our HOD, Prof. SYED KALIM, for providing us his/her guidance from time to time. His/her encouragement proved to be a boon in the path of our achievement.

We are thankful to our guide, Prof. SYED KALIM for giving us valuable inputs for the development of our project.

Last but not the least we also thank our lab technicians and all the non-teaching staff.
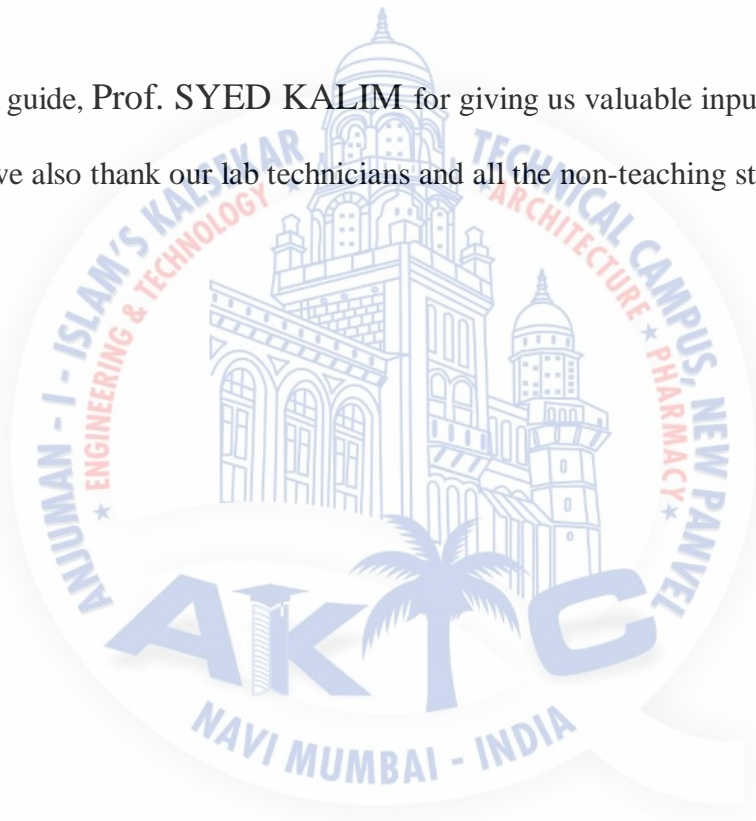
ABSTRACT

This thesis deals with airplanes using solar energy as their only source of energy for more than 24 hours flight. Using solar panels, they collect it during the day for immediate use but also store the remaining part for the night flight. This work presents a new analytical methodology for the conceptual design of such airplane. Its major advantage lies in the fact that it is simple and versatile, which makes it applicable to a large range of airplanes of different wingspans, from the small MAV to the large manned aircraft.

The ability to produce power without damaging the Environment is a continuing challenge Fossils fuels like Gasoline natural gas and coal, all come from Non-renewable sources and when burned, increase the Level of air pollution and may harm the environment. Batteries, such as those found in flashlight and MP3 Players, have limited lifetimes and often end up being disposed of in landfills. There are many environmental friendly alternative available today such as wind energy, geothermal, hydroelectric power plant and finally solar energy. The Sun emits a tremendous amount of energy every second of every day. Only a very small fraction of the Sun's energy ever makes it to the Earth, but it's still an incredibly large amount. A lot of that energy is already used in the form of heat, or by plants needing the light for photosynthesis, converting carbon dioxide into sugars and eventually releasing breathable oxygen, but it still leaves a large portion un-used and ready for capture. Solar aircraft is one of the ways to utilize solar energy. Solar aircraft uses solar panel to collect the solar radiation for immediate use but it also store the remaining part for the night flight. This paper intended to stimulate research on renewable energy sources for aviation. In future solar powered airplanes could be used for different types of aerial monitoring and unmanned flights. This synopsis briefly shows history, application, working, advantages, and disadvantage of solar aircraft and concludes by stating the need to utilize free solar energy for aviation.

Key words: Solar powered UAV, Solar Energy, Solar Airplane, Sustainable Flight, mini impulse, MPPT, Conceptual Design Methodology

TABLE OF CONTENTS

CHAPTER 1

1.Introduction

1.1 Motivations and Objectives

The ability for an aircraft to fly during a much extended period of time has become a key issue and a target of research, both in the domain of civilian aviation and unmanned aerial vehicles. This latter domain takes an increasingly important place in our society, for civilian and unfortunately military applications. The required endurance is in the range of a couple of hours in the case of law enforcement, border surveillance, forest fire fighting or power line inspection. However, other applications at high altitudes, such as communication platform for mobile devices, weather research and forecast, environmental monitoring, would require remaining airborne during days, weeks or even months.

For the moment, it is only possible to reach such ambitious goals using electric solar powered platforms. Photovoltaic modules may be used to collect the energy of the sun during the day, one part being used directly to power the propulsion unit and onboard instruments, the other part being stored for the night time. In order to reach the target endurance, the design of the airplane has to be thought carefully and globally, as a system composed of many subsystems that are continuously exchanging energy. Due to these relationships, each

part has to be sized accordingly to all the others. Here, the design method is to engineering what the recipe is to cooking. A good chef can cook an exceptional meal with standard products, whereas his apprentice can miss it completely even using expensive high quality products. Simply because a crucial part lies in the combination of all the elements, and not only in their quality. This is especially true for multidisciplinary projects, the case of a solar airplane being an ideal example as it requires knowledge in the fields of aerodynamics, actuators, sensors, electronics, energy storage, photovoltaic, etc.

In 2004, the Autonomous Systems Lab of EPFL/ETHZ started the Sky- Sailor project, under a contract with the European Space Agency. ESA had the vision to send to Mars an airplane that could achieve various scientific

missions. Compared to other airplane concepts for planetary missions, like AME (Airplane for Mars Exploration) [63] or ARES (Aerial Regional-scale Environmental Survey) [67] that would be capable of embedding several kilograms for missions limited to a few hours, the goal was here to embed a

payload of less than half a kilogram but for missions of weeks, even months, using solar energy. So the target was to study the feasibility of a solar powered airplane aimed at flying continuously in the atmosphere of Mars. As a first step, the feasibility of continuous flight on Earth was to be studied, with the idea to fly an Earth prototype at altitudes where similarities occur with the red planet.
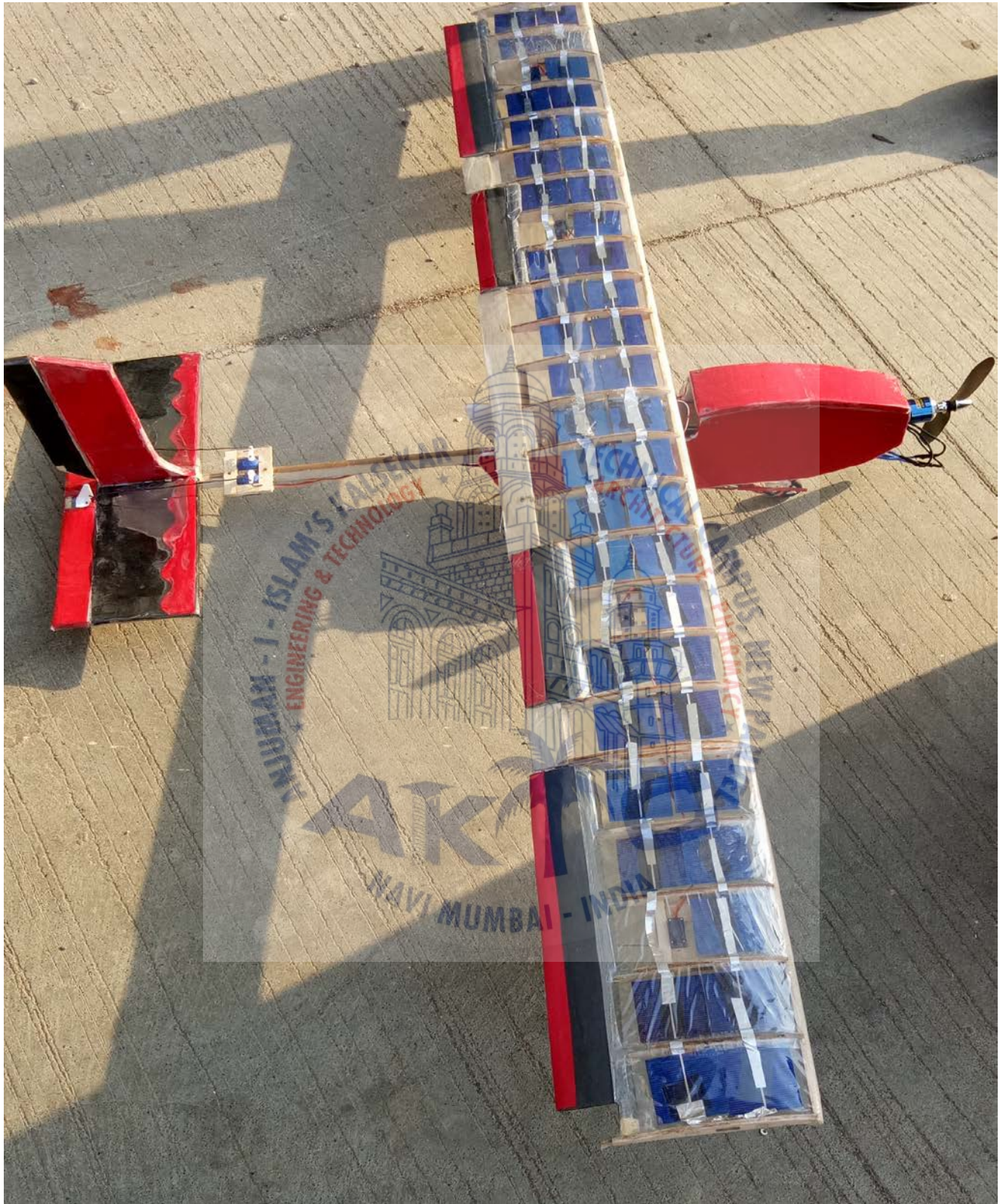
Figure 1.1: The fully functional solar airplane prototype

1.2 History of Solar Powered Flight

1.2.1 The Conjunction of two Pioneer Fields, Electric Flight and Solar Cells

The use of electric power for flight vehicles propulsion is not new. The first one was the hydrogen-filled dirigible France in year 1884 that won a 10 km race around Villacoulbay and Medon. At this time, the electric system was superior to its only rival, the steam engine, but then with the arrival of gasoline engines, work on electrical propulsion for air vehicles was abandoned and the field lay dormant for almost a century . On the 30th of June 1957, Colonel H. J. Taplin of the United Kingdom made the first officially recorded electric powered radio controlled flight with his model "Radio Queen", which used a permanent-magnet motor and a silverzinc

battery. Unfortunately, he didn't carry on these experiments. Further developments in the field came from the great German pioneer, Fred Militky, who first achieved a successful flight with an uncontrolled model in October 1957. Since then, electric flight continuously evolved with constant improvements in the fields of motors and batteries .

Three years before Taplin and Militky's experiments, in 1954, photovoltaic technology was born at Bell Telephone Laboratories. Daryl Chapin, Calvin Fuller, and Gerald Pearson developed the first silicon photovoltaic cell capable of converting enough of the sun's energy into power to run everyday electrical equipment. First at 4 %, the efficiency improved rapidly to 11% . Two more decades will be necessary to see the solar technology used for the propulsion of electric model airplanes.

1.2.2 Early Stages of Solar Aviation with Model Airplane

On the 4th of November 1974, the first flight of a solar powered aircraft took place on the dry lake at Camp Irwin, California. Sunrise I, designed by R.J. Boucher from Astro Flight Inc. under a contract with ARPA, flew 20 minutes at an altitude of around 100m during its inaugural flight. It had a wingspan of 9.76 m, weighed 12.25 kg and the power output of the 4096 solar cells was 450W [33]. Scores of flight for three to four hours were made during the winter, but Sunrise I was seriously damaged when caught flying in a sand storm. Thus, an improved version, Sunrise II, was built and tested on the 12th of September 1975. With the same wingspan, its weight was reduced to 10.21 kg and the 4480 solar cells were able this time to deliver 600W thanks to their 14% efficiency. After many weeks of testing, this second version was also damaged due to a failure in the command and control system. Despite all, the history of solar flight was engaged and its first demonstration was done.

Figure 1.2: Sunrise I (1974)

On the other side of the Atlantic, Helmut Bruss was working in Germany on a solar model airplane in summer 1975 without having heard anything about Boucher's project. Unluckily, due to overheating of the solar cells on his model, he didn't achieve level flight and finally the first one in Europe was his friend Fred Militky, one year later, with Solaris. On the 16*th* of August 1976, it completed three flights of 150 seconds reaching the altitude of 50m [38]. Since this early time, many model airplane builders tried to fly with solar energy, this passion becoming more and more affordable. Of course, at the beginning, the autonomy was limited to a few seconds, but it rapidly became minutes and then hours. Some people distinguished themselves like Dave Beck from Wisconsin,

USA, who set two records in the model airplane solar category F5 open SOL of the FAI [21]. In August 1996, his Solar Solitude flew a distance of 38.84km in straight line and two years later, it reached the altitude of 1283m [18,21]. The master of the category is still Wolfgang Schaeper who holds now all the official records : duration (11 h 34mn18 s), distance in a straight line (48.31 km), gain in altitude (2065 m), speed (80.63 km/h), distance in a closedcircuit (190 km) and speed in a closed circuit (62.15 km/h). He achieved these performances with Solar Excel from 1990 to 1999 in Germany [15].

1.2.3 The Dream of Manned Solar Flight

After having flown solar model airplanes and proved it was feasible with sufficient illumination conditions, the new challenge that fascinated the pioneers at the end of the 70's was manned flights powered solely by the sun.

On the 19th of December 1978, Britons David Williams and Fred To launched Solar One on its maiden flight at Lasham Airfield, Hampshire

121]. First intended to be human powered in order to attempt the Channel crossing, this conventional shoulder wing monoplane proved too heavy and thus was converted to solar power. The concept was to use nickel-cadmium battery to store enough energy for short duration flights. Its builder was convinced that with high-efficiency solar cells like the one used on Sunrise, he could fly without need of batteries, but their exorbitant price was the only limit.

On April 29, 1979, Larry Mauro flew for the first time the Solar Riser, a solar version of his Easy Riser hang glider, at Flabob Airport, California. The 350Wsolar panel didn't have sufficient power to drive the motor directly and was here again rather used as a solar battery

charger. After a three hours charge the nickel-cadmium pack was able to power the motor for about ten minutes. His longest flight covered about 800m at altitudes varying between 1.5m and 5m [33].

This crucial stage consisting in flying with the sole energy of the sun without any storage was reached by Dr. Paul B. McCready and AeroVironment Inc, the company he founded in 1971 in Pasadena, California. After

having demonstrated, on August 23, 1977, sustained and maneuverable human-powered flight with the Gossamer Condor, they completed on June 12, 1979 a crossing of the English Channel with the human-powered Gossamer Albatross. After these successes, Dupont sponsored Dr. MacCready in an attempt to modify a smaller version of the Gossamer Albatross, called Gossamer Penguin, into a man carrying solar plane. R.J. Boucher, designer of Sunrise I and II, served as a key consultant on the project. He provided the motor and the solar cells that were taken from the two damaged versions of Sunrise. On the 18th of May 1980, the Gossamer Penguin, with 13 years old MacCready's son Marshall on board, realized what can be considered as the world's first piloted, solar powered flight.

Figure 1.4: Gossamer Penguin (1980)

1.2.4 On the Way to High Altitude Long Endurance Platforms and Eternal Flight After the success of Solar Challenger, the US government gave funding to AeroVironment Inc. to study the feasibility of long duration, solar electric flight above 19812km (65000ft). The first prototype HALSOL proved the aerodynamics and structures for the approach, but it suffered from its

for energy storage, that were inadequate for this type of mission. Thus, the project took the direction of solar propulsion with the Pathfinder that achieved its first flight at Dryden in 1993. When funding for this program ended, the 30m wingspan and 254kg aircraft became a part of NASA's Environmental Research Aircraft Sensor Technology (ERAST) program that started in 1994. In 1995, it exceeded Solar

Challenger's altitude record for solar powered aircraft when it reached 15392m(50500ft) and two years later he set the record to 21802m (71530ft). In 1998, Pathfinder was modified into a new version, Pathfinder Plus, which had a larger wingspan and new solar, aerodynamic, propulsion and system technologies. The main objective was to validate these new elements before building its successor, the Centurion. Centurion was considered to be a prototype technology demonstrator for a future fleet of solar powered aircrafts that could stay airborne for weeks or months achieving scientific sampling and imaging missions or serving as telecommunications relay platforms [17]. With a double wingspan compared to Pathfinder, it was capable to carry 45kg of remote sensing and data collection instruments for use in scientific studies of the Earth's environment and also 270kg of sensors, telecommunications and imaging equipment up to 24400m (80000ft) altitude. A lithium battery provided enough energy to the airplane for two to   five hours flig

Figure 1.7: Centurion (1997-1999) and Helios (1999-2003)

The last prototype of the series designated as Helios was intended to be the ultimate"eternalairplane",incorporatingenergystoragefornight-timeflight. For NASA, the two primary goals were to demonstrate sustained flight at an altitude near 30480m (100000ft) and flying non-stop for at least 24 hours, includingatleast14hoursabove15240m(50000ft). In2001,Heliosachieved the first goal near Hawaii with an uno   fficial world ltitude of 29524m (96863ft) and a 40 minutes flight above 29261m (96000ft). Unfortunately, it never reached the second objective as it was destroyed when it fell into the Pacific Ocean on June 26, 2003 due to structural failures.

Solar Impulse is a Swiss long-range experimental solar-powered aircraft project, and also the name of the project's two operational aircraft.[2] The privately financed project is led by Swiss engineer and businessman André Borschberg and Swiss psychiatrist and balloonist Bertrand Piccard, who co-piloted *Breitling Orbiter 3*, the first balloon to circle the world non-stop.[3] The Solar Impulse project's goals were to make the first circumnavigation of the Earth by a piloted fixed-wing aircraft using only solar power and to bring attention to clean technologies.[4]

The aircraft are single-seat monoplanes powered by photovoltaic cells; they are capable of taking off under their own power. The prototype, often referred to as *Solar Impulse 1*, was designed to remain airborne up to 36 hours.[5] It conducted its first test flight in December 2009. In July 2010, it flew an entire diurnal solar cycle, including nearly nine hours of night flying, in a 26-hour flight.[6] Piccard and Borschberg completed successful

solar-powered flights from Switzerland to Spain and then Morocco in 2012,[7] and conducted a multi-stage flight across the US in 2013.[8][9]

A second aircraft, completed in 2014 and named **Solar Impulse 2**, carries more solar cells and more powerful motors, among other improvements. On 9 March 2015, Piccard and Borschberg began to circumnavigate the globe with *Solar Impulse 2*, departing from Abu Dhabi in the United Arab Emirates.[10] The aircraft was scheduled to return to Abu Dhabi in August 2015 after a multi-stage journey around the world.[11] By June 2015, the plane had traversed Asia,[12] and in July 2015, it completed the longest leg of its journey, from Japan to Hawaii.[13] During that leg, the aircraft's batteries sustained thermal damage that took months to repair.[14] *Solar Impulse 2* resumed the circumnavigation in April 2016, when it flew to California.[15][16] It continued across the US until it reached New York City in June 2016.[17] Later that month, the aircraft crossed the Atlantic Ocean to Spain.[18] It stopped in Egypt[19] before returning to Abu Dhabi on 26 July 2016, more than 16 months after it had left, completing the approximately 42,000 kilometre (26,000 mile) first circumnavigation of the Earth by a piloted fixed-wing aircraft using only solar power

CHAPTER 2
Basic Concepts

2.1 Introduction

In this chapter, we briefly explain the basic principles that make a solar airplane fly and especially the technologies that are involved. Only the theory that is needed to understand the design in the next chapter is discussed.

References allow the reader who wants to dig deeper in a subject to do so. Like all other airplanes, a solar airplane has wings that constitute the lifting part. During steady flight, the airflow due to its relative speed creates two forces : the lift that maintains the airplane airborne compensating the weight and the drag that is compensated by the thrust of the propeller.
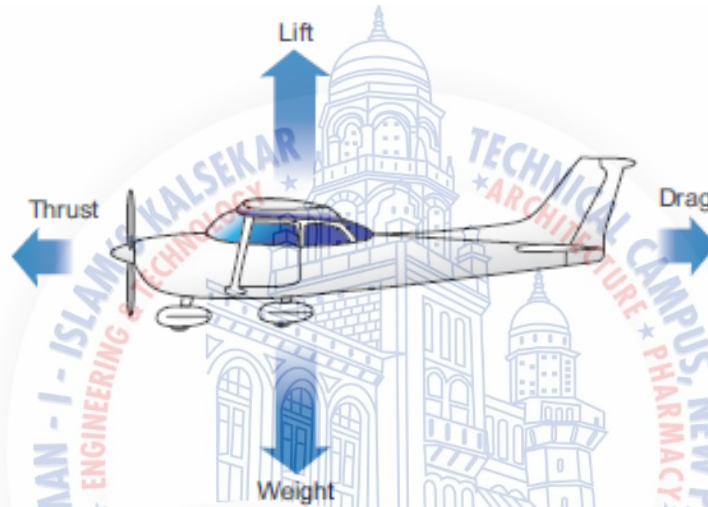
Figure 2.1: Forces acting on an airplane at level flight

The solar panels, composed by solar cells connected in a defined configuration, cover a given surface of the wing or potentially other parts of the airplane like the tail or the fuselage. During the day, depending on the sun irradiance and elevation in the sky, they convert light into electrical energy. A converter ensures that the solar panels are working at their maximum power point. That is the reason why this device is called a Maximum Power Point Tracker, that we will abbreviate MPPT. This power obtained is used firstly to supply the propulsion group and the onboard electronics, and secondly to charge the battery with the surplus of energy.
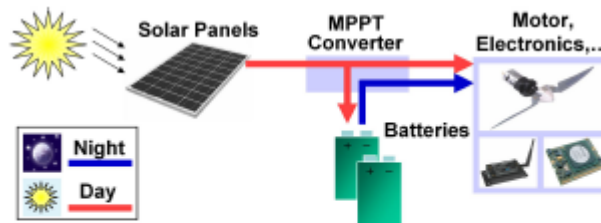
Figure 2.2: Solar airplane basic principle

During the night, as no more power comes from the solar panels, the various elements consuming energy are supplied by the battery that has to last until the next morning where a

new cycle starts. After the description of this general concept, we will approach the theory of the different parts separately in the next sections.

2.2 Aerodynamics of a Wing

Figure 2.3 shows the cross section of a wing in a laminar airflow with a constant speed v. The circulation of this airflow creates a different pressure distribution on the upper and lower side of this section that once integrated
can be represented as two forces, the lift and the drag.
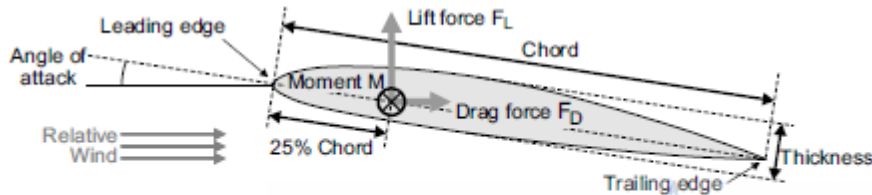
Figure 2.3: Section of an airfoil

These forces can be calculated using the following equations :

$$F_L = C_L \frac{\rho}{2} S v^2$$

$$F_D = C_D \frac{\rho}{2} S v^2$$

Where C_L and C_D are respectively the lift and drag coefficients, _ is the air density, S the wing area and v the relative airspeed. The C_L and C_D heavily depend on the airfoil, the angle of attack and the Reynolds number Re which is representative of the air flow viscosity.
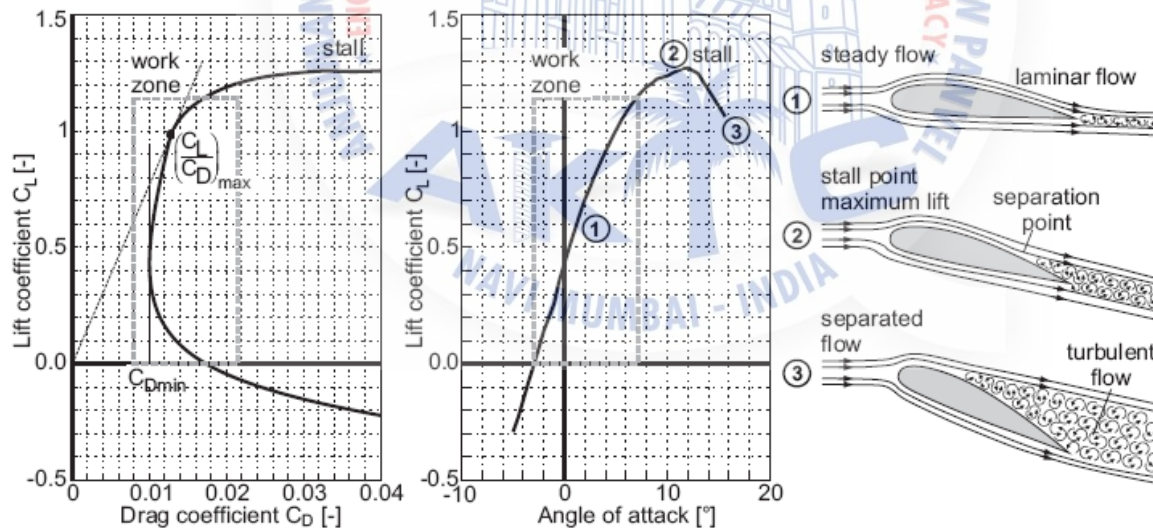
Figure 2.4:

Lift and drag coefficients depending on the angle of attack
    What was depicted so far is the case of an infinite length wing, but for a real wing, vortices are produced at the wing tips, which induce an additional drag called the induced drag. It represents the energy spent for producing the wake behind the wing and follows :

$$C_{D\,ind} = \frac{C_L^2}{e\pi AR}$$

AR is the aspect ratio, i.e. the ratio between the wingspan b and the chord length c that can also be expressed with the wing area using $AR = b/c = b_2/(bc) = b_2/S$. The variable e is the Oswald efficiency factor that has a value between 0 and 1, 1 being the ideal case where the load distribution on the wing is elliptical. In many cases, its value is between 0.75 and 0.85. This induced drag has to be taken into account especially for small aspect ratios airplane as it becomes more important. Finally, there is the parasitic drag coming from non-lifting parts, like the fuselage or the tail. The final drag coefficient is thus the sum of them.

$$C_D = C_{D\,afl} + C_{D\,ind} + C_{D\,par}$$

2.3 Solar Cell
A solar cell or photovoltaic cell is a device that converts solar energy into electricity by the photovoltaic effect. It is very widely used in space application because it allows a clean and long-duration source of energy requiring almost no maintenance. Solar cells are composed of various semiconducting materials, constituting one or more layers. Silicon is very often used as it is the second most abundant element in Earth's crust and thus inexpensive. For this reason, this material will be considered in the further explanations that are also valid for other types of semiconductors.

2.3.1 Working Principles
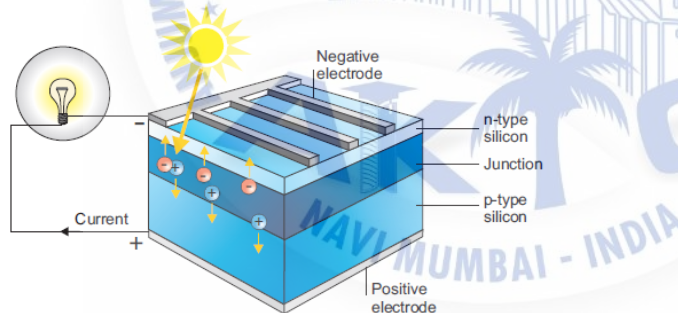
Figure 2.5: Working principle of a solar cell (Source : http://www.renewables-made-in-germany.com/en/photovoltaik/)

In figure 2.5, a simple silicon solar cell is represented with two doped semiconductors layers, p-type and n-type. When the sunlight strikes the solar cell surface the cell creates charge carriers as electrons and holes. The internal field produced by junction separates some of the positive charges (holes) from the negative charges (electrons). The holes are swept into the positive or player and the electrons are swept into the negative or n-layer. When a circuit is made, the free electrons have to pass through the load to recombine with the positive holes, current can be produced from the cells under illumination.

2.3.2 Solar Irradiance
The energy coming from the sun depends on the wavelength, leading to the solar spectrum

represented in figure 2.6. The reference solar spectral irradiance AM0 (Air Mass 0) represents the irradiance at the top of the atmosphere with a total energy of 1353W/m2. At sea level, it is referred as AM1.5 and the total energy equals 1000W/m2. In addition to the direct irradiance, we also have to consider the diffuse irradiance, which is predominant on a cloudy day, and the reflected irradiance. Reflected irradiance is dependent on the albedo, which is a measure of the reflectivity of the Earth's surface. Fresh snow has an albedo of around 80 %, desert sand 40% and grass between 5% and 30 %.
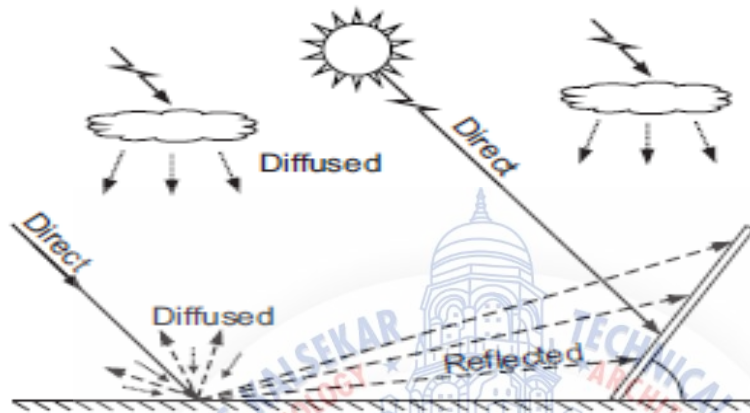
Figure 2.7: Direct, diffuse and reflected irradiance [71]

2.3.3 Types of Solar Cells

There exist various types of photovoltaic cells that can be sorted according to the type of material, the fabrication process, substrate, etc. The objective here is only to give a short and non-exhaustive overview of the existing types. The reader can refer to [82] for deeper information. The most widely used type of material is silicon, because of its abundance and low cost. We can distinguish three types of *silicon solar cells* according

to the type of crystal :

• monocrystalline, for which absolutely pure semiconducting material is
used which gives a high level of efficiency but at a high cost.

• polycrystalline, composed of crystal structures of varying sizes. The
manufacturing process is more cost efficient but leads to less efficient
solar cells.

• amorphous, or thin-layer cell, where a silicon film is deposited on glass
or another substrate material, even flexible. The thickness of this layer
is less than 1 μm, thus the production costs are very low, but the efficiency
is poor as well.

However, other materials can be used as well like elements from groups three to five of the periodic table of the elements to produce *compound solar cells*. These include gallium arsenide, copper indium diselenide, cadmium telluride, etc. These cells are more expensive to produce, but lead to higher efficiency. We can also mention the *polymer solar cells* made of organic material and the *dye sensitized solar cells* that are very promising technologies because they are inexpensive to fabricate. However, these technologies suffer from unstable efficiency problems that still must be solved and are not yet viable for industry.

In fact, the most efficient solar cells are of a stack of individual singlejunction cells in descending order of bandgap. The top cell captures highenergy photons and passes the rest on to lower-bandgap cells. These multijunction cells can then convert a wider part of the solar spectrum of figure 2.6 leading to a high efficiency that goes up to 40 %. Figure 2.8 shows the best efficiencies obtained for various solar cell technologies.

2.3.4 Current and Voltage of a Solar Cell

The current to voltage curve of a solar cell has a very characteristic shape and can be described by the mathematical models of an ideal or real photovoltaic generator that will not be developed here but can be found in [78]. As depicted in figure 2.9, when the cell pads are not connected, no current is produced and the voltage equals V_{OC}, the open circuit voltage. When it is short circuited, the voltage is zero but the current equals I_{SC}. In between these two points where in both cases the power retrieved is zero, there is a working point, called the maximum power point, where the power one can retrieve is the highest and equals $P_{max} = V_{MPP} I_{MPP}$. It is precisely at this point that the cells should be used and the ratio between P_{max} and the light intensity represents precisely the efficiency of the solar cell. However, the curve, and thus this point, is not fixed and varies depending on many parameters.
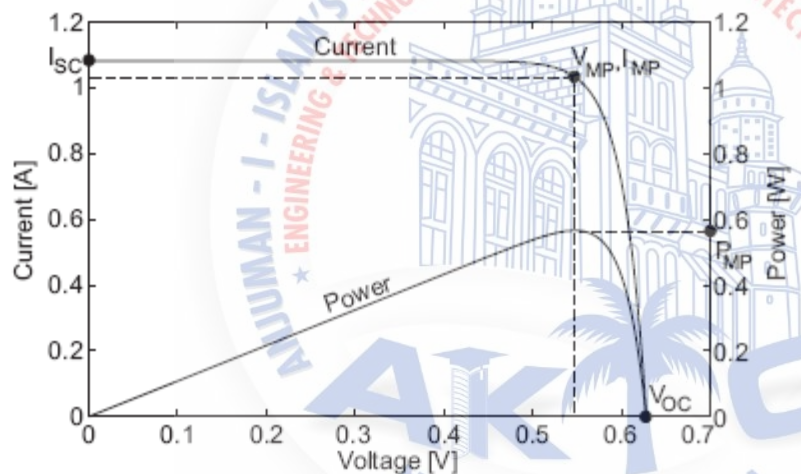
Figure 2.9: Current to voltage curve of a solar cell

The current of a solar cell is proportional to its area and varies almost linearly with the light intensity (Figure 2.10). The voltage varies only a little bit when the light intensity changes and is independent of the cell surface, but depends on the semiconductor material. For a single layer silicon cell, V_{MPP} is around 0.5 V, but for a triple junction gallium arsenide cell, it increases up to 2.27 V. The important values of V_{OC}, I_{SC}, V_{MPP}, I_{MPP} are given in solar cells datasheets under standard spectrum conditions, either AM0 or AM1.5, that were presented previously.

Temperature also affects the characteristics of solar cells. When it increases, the voltage decreases slightly whereas the current increases insignificantly. Globally, the power that a solar cell can give is higher for lower temperature, considering the same irradiance conditions (Figure 2.10).

An assembly of solar cells connected electrically in parallel, which increases the current, or in series, increasing then the voltage, is referred to as a solar module or solar panel. The I-V curve of a solar module has a scaled but similar shape to that of the single cell curve.

2.4 Energy Storage

When the energy production is not constant and continuous, a good energy storage method is necessary. We can list many different ways to store energy

• Chemical (hydrogen, biofuels)

• Electrochemical (batteries, fuel cells)

• Electrical (capacitor, supercapacitor, superconducting magnetic energy storage or SMES)

• Mechanical (compressed air, flywheel)

• Thermal

These different technologies coexist because their characteristics make them attractive to different applications. From a user point of view, the main selection criteria are the energy and power density, the response time,

the lifetime, the efficiency and of course the costs. In the case of a solar airplane, the gravimetric energy density in Wh/kg, also called specific energy, and the peak power are the most crucial parameters that determine the choice of the energy storage method. The volumetric energy density will of course also have an influence on the fuselage size, but this volume plays a minor role on the power required compared to the weight. A look at figure 2.11 shows that in the present case, electrochemical batteries and fuel cells are the two best candidates. In fact, they have the highest gravimetric energy density from all the solutions that are reversible.

Working Principles

Electrochemical batteries are energy storage devices, which are able to convert chemically stored energy into electrical energy during discharging. They are composed of a cathode and an anode, made of two dissimilar metals, that are in contact with an electrolyte. When all elements are in contact with each other, a flow of electron is produced. If the process is reversible so that they can be recharged, they are referred to as secondary batteries, in the other case they are primary batteries [97]. Concerning a solar airplane, rechargeable batteries will of course be used.

Several technologies are available and currently, the lithium-ion (or lithiumion-polymer where the electrolyte is a gel and not a liquid) technology is the best concerning gravimetric energy density, compared to lead-acid, nickelcadmium (NiCd) or nickel-metal-hydride (NiMH). The nominal voltage of a lithium-ion cell is 3.7V compared to 1.2V for NiCd and NiMH and its capacity, in Ah depends on its size.

Charge and Discharge Process of a Lithium-Ion Battery

The charging process of lithium-ion batteries is quite simple, but has to be done very carefully because of safety reasons. During a first phase, a constant current charges the battery while the voltage increases as depicted in figure 2.12. Once 4.2V is reached, the second phase starts during which the voltage is kept constant while the current accepted by the cell slowly decreases. When this current is below 5% of the maximum current, the battery is charged. The maximum charge rate, depending on the manufacturer, is always lower than 1 C, where C stands for the capacity of the battery. Considering a cell with a capacity of 800mAh, 1C represents a current of 800mA during one hour, 0.5C gives 400mA during 2 hours, etc. For this reason, lithiumion cells always need a minimum of one hour to be charged. Concerning the charging voltage, it should never exceed 4.2 V. Using a charge rate higher than 1C or overcharging above the maximum voltage damages the cell and potentially results in explosion and/or fire.

Concerning the discharge process, the maximum discharge current is specific to each model. Batteries with high discharge rates of around 20C are

available, but the models that offer a high gravimetric energy density are always rated to less than 1C. At the end of the discharge, the voltage drops very fast below 3 V, as seen in figure 2.13. At this moment, the load has to be removed as soon as the voltage reaches approximately 2.7V per cell, or else the battery will subsequently no longer accept a full charge and may experience problems holding voltage under load.

2.4.2 Fuel Cells

A fuel cell is a system where the chemical energy of reactants, often a gaseous fuel and the oxygen in the atmosphere, is converted directly into electrical energy and heat. It is the equivalent of burning the fuel; however, as the energy is directly converted to electricity, it is more efficient. What is called the fuel cell is only the part where the reaction and the conversion occurs. It doesn't include the reactants that are stored in separated tanks.

Thank to its high gravimetric energy density, hydrogen is the most favored and common fuel used, that is the reason why we will consider it for the following explanation. The fuel cell consists of two electrodes, known as the anode and cathode that are separated by an electrolyte (Figure 2.15). Oxygen is passed over the cathode and hydrogen over the anode. Hydrogen ions are formed together with electrons at the anode. The hydrogen ions migrate to the cathode through the electrolyte and the electrons produced at the anode flow through an external circuit to the cathode. At the anode they combine with oxygen to form water. The flow of electrons through the external circuit provides the current of the cell.

The great advantage is that the combustion of hydrogen with oxygen produces only water, which is not a pollutant, and that hydrogen has also a
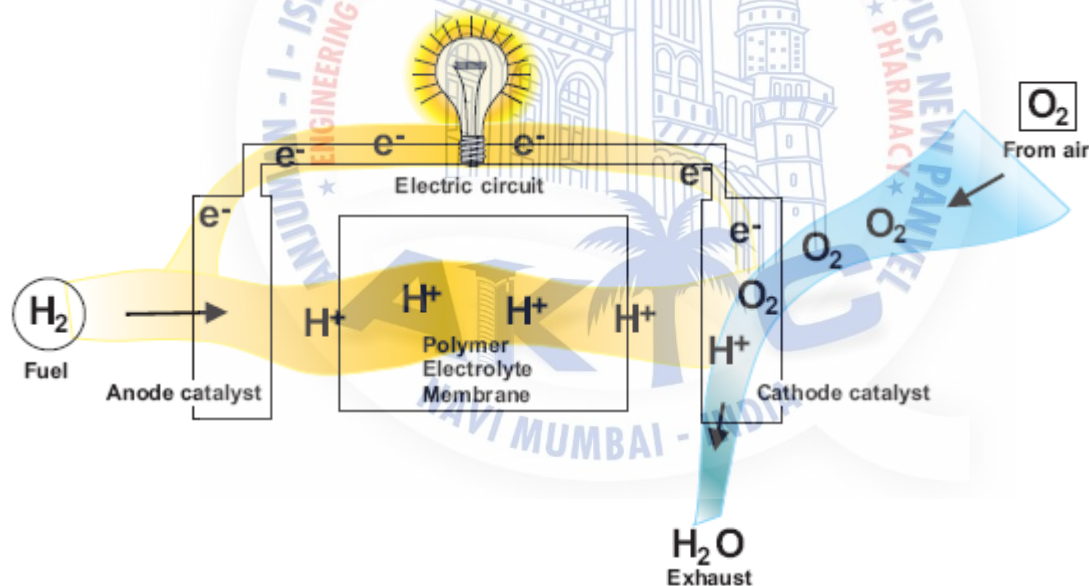
Figure 2.15: Working principle of a fuel cell

Table 2.1 establishes a list of commonly used fuels with their energy density, sugar being given just as an interesting comparison point. Of course, we have to keep in mind that the problem of hydrogen is that it is not present in nature but can be obtained through the electrolysis of water, and that at atmospheric pressure, its volumetric energy density is very low.

At a first glance, the 33.3 kWh/kg of hydrogen makes the 0.2 kWh/kg of lithium-ion batteries seen above look ridiculous, but this is a wrong comparison. In fact the whole system that converts this chemical energy into electricity is constituted by the hydrogen compressed in a tank, the fuel cell stack, pumps, filters, valves, pressure transducers, etc. All these elements

mean additional weight compared to the hydrogen only and losses, taking
into account that all the pumps, valves and control electronics require power.
There are different types of fuel cells, varying with the type of electrolyte
and fuel, but the more suitable for solar powered airplane are the PEM
(Proton Exchange Membrane or Polymer Electrolyte Membrane) fuel cells,
because they have a fast start and response time, are compact and operate
at low temperature (80 _C). Their disadvantages are that they are still very
expensive because of the platinum they use, have a poor efficiency and their
lifetime and reliability are still to be improved.

However, if we want to use a fuel cell on a solar airplane to store the
energy during the day and reuse it during the night, not only the generation
of electricity from hydrogen and oxygen has to be realized on the plane, but
also the reverse reaction where the cell act as an electrolyzer, electricity and
water being combined to create oxygen and hydrogen. This dual-function
system is known as a reversible or unitized regenerative fuel cell (URFC).
Since the beginning of the 90's, the Lawrence Livermore National Laboratory
is a world leader in this field, especially under the lead of Fred Mitlitsky
[84]. The collaboration with the NASA on the Pathfinder, Pathfinder
Plus and Helios solar airplanes oriented the research efforts not only in the direction
of efficiency but also towards very low weight [86]. Militsky achieved a
packaged specific energy of 400 to 1000Wh/kg for an URFC with lightweight
pressure vessels [85]. A lot of work has to be done on the round trip efficiency,
which is the product of the charge and discharge efficiencies. While
the theoretical round-trip efficiency of regenerative H_2/O_2 fuel cells is about
80 %, practically achievable efficiencies hardly reached 50% [29, 61]. The
hydrogen-bromine regenerative fuel cells offer an efficiency of up to 80% [76]
and research is still going on. So, there will certainly be many improvements
in the gravimetric energy density, efficiency and hopefully miniaturization of
fuel cells in the future decades.

2.5 Maximum Power Point Tracker

As described in section 2.3, a solar cell has a working point on its current
to voltage curve where the power retrieved is maximal. In order to work at
this point, which is continuously moving because of the constantly changing
irradiance conditions, and thus get the highest amount of energy, a so called
Maximum Power Point Tracker (MPPT) is required. An MPPT is basically
a DC/DC converter with variable and adjustable gain between the input
and the output voltage, the input being the solar panels and the output the
battery. It contains electronics that monitor both the current and the voltage
on each side, which allows a determination for how the gain has to be changed
to ensure the best use of the solar panels.

There are different algorithms to track this maximum power point. One
very well known is called the "Hill Climbing" method; considering a constant
battery voltage, which is valid at short term, increasing/decreasing the voltage
gain makes the working point, on the power curve of figure 2.9, move
respectively to the left/right. The current and voltage are measured to compute
the actual power. If it is higher than the previous power, the direction of
movement is kept as one is getting more energy, if not, direction is changed.
A consequence is that the working point is never at the MPP, but oscillating
around it, giving thus an average power slightly below the maximum power.
This tracking function operates only during the first phase of the battery
charge, when the voltage is below the maximal value that would destruct the
lithium-ion cells (4.23 V/cell). In the second phase, i.e. constant voltage,
decreasing current, the power has to be reduced below MPP. That means
that the tracking is still executed, but with an additional condition that if
the voltage approaches the maximum, the direction is automatically changed,

reducing the power.
As part of the energy chain, the MPPT has to be as efficient as possible.
Thus, not only the hardware design has to be optimized to minimize the
losses in diodes, transistors and inductors, but also the algorithm has to be
tuned to have a fast adaptation to irradiance variations and a good tracking
precision. A well designed MPPT should have an efficiency above 95%, but
the best products reach 99 %.

2.5 Electric Motor

An electric motor uses electrical energy to produce mechanical energy. This definition is very general
and in fact there exist a very large variety of electric motors that coexist because of the different supply
sources, sizes, torques and speeds depending on the application. In the present case, DC (Direct Current
or Continuous Current) motors will be used as they are designed to run on DC electric power supplied
by a battery. By far the most common types are the brushed and brushless types, which use mechanical
and electronic commutation respectively to create a rotating magnetic field vector that pulls an
electromagnet or a permanent magnet. In a classic DC motor, the inner part is the rotor, which consists
of a wound coil generating a rotating magnetic field, and the outer part is either an electromagnet or
permanent magnet stator, which creates a fixed magnetic field. The electrical connection between the
rotor and the external power supply are ensured by brushes. Hence, the rotation will continuously
change the coil polarity, thus generating an oscillating current. This current is at the origin of the rotating
magnetic field and the turning moment. The limitations of DC motors are due to the need for brushes to
press against the commutator what creates friction, sparks and electrical noise, especially as currents and
speeds get higher. Also, the windings induce a high inertia to rotate and as they are placed in the center
of the motor, they have trouble getting rid of the heat due to the Joule effect. In order to have high
efficiency, a precision assembly and good components are required. Anyway, their speed control is
easily achieved by varying the constant voltage or the duty cycle of a Pulse Width Modulated signal
(PWM).
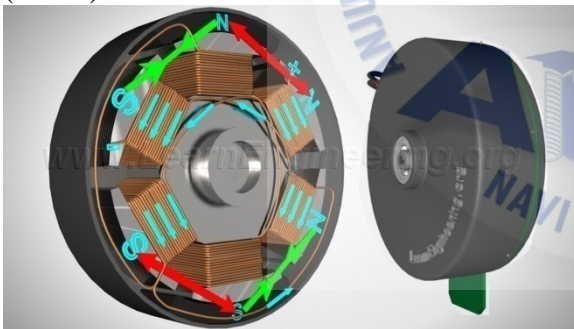
In a brushless DC motor, often abbreviated BLDC, the coils do not move. Instead, the permanent
magnets rotate and the armature remains static. This gets around the problem of how to transfer current
to a moving armature.
In order to do this, the brush-system/commutator assembly is replaced by an electronic controller that
performs the same power distribution found in a brushed DC motor. The drive electronics is more
complex that for
brushed motors because it has to activate the coils one phase after the other,what has to be synchronized
to the rotor's position. In order to sense the position, either Hall Effect sensors or Back Electro Magnetic
Force (BEMF) are used. When configured with the magnets on the outside, they are referred to as
outrunner motors, else they are called inrunner. The advantages of BLDC motors are numerous : very
precise speed control, high efficiency, reliability, reduced noise, longer lifetime (no brush abrasion), no

ionizing sparks. Additionally, they run much cooler than brushed motors which allows the use of higher currents. For this reason, their power to weight ratio is exceptionally high.

2.6 Propeller

The propeller is a device consisting of a set of two or more twisted, airfoilshaped blades mounted around a shaft and spun to provide propulsion of a vehicle through a fluid. It accelerates incoming air particles creating a reaction force called thrust. If we consider a stream tube around it, as the mass of air passing through the stream tube must be constant, the increased velocity leads to a contraction of the stream tube passing through the propeller disk, neglecting compressibility.

In order to better understand how it works, we will present the Blade Element Theory (BET) that gives basic insight into the rotor performanceas well as other characteristics. In this theory the blade is assumed to be composed of numerous, infinitesimal strips with width 'dr' that are connected from tip to tip. The lift and drag are estimated at the strip using the 2-D airfoil characteristics of the section. Also, the local flow characteristics are accounted for in terms of climb speed, inflow velocity, and angular velocity. The section lift and drag may be calculated and integrated over the blade span. The propeller efficiency n_{plr} is defined as the ratio between the propeller thrust T times the propeller axial speed v and the resistance moment M_{plr} times the rotational speedN.

(a)   (b)
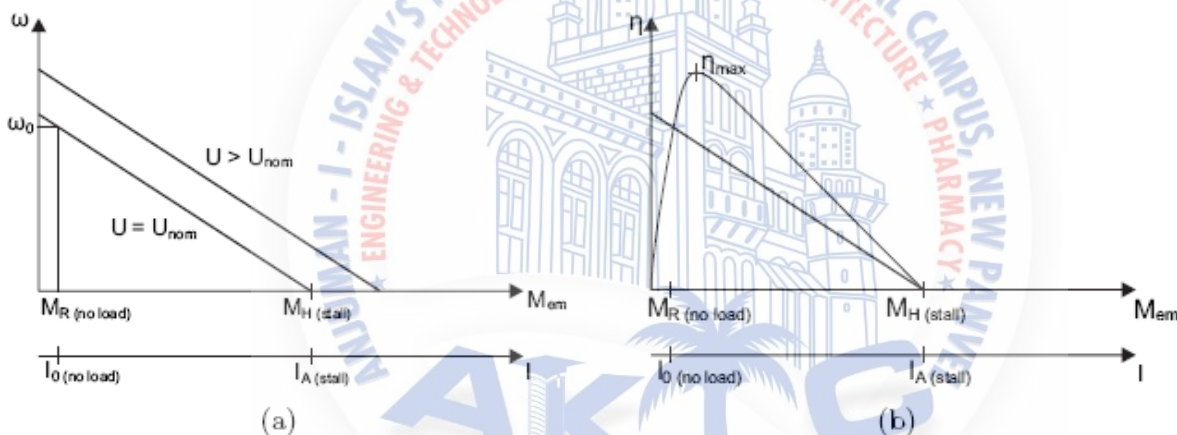
So designing an efficient propeller comes to the same challenges as for an airplane wing : find the best airfoil, chord and incidence angle that minimize the resistance torque and maximize the thrust for a given axial speed. This optimum varies along the blade, from the hub to the tip, due to the increasing radius and thus airspeed, explaining the twisting shape of propellers. A

$$\eta_{plr} = \frac{T\,v}{M_{plr}\,\omega}$$

good propeller designed for a specific flight domain should have an efficiency of at least 80%, 85% being an excellent value that is difficult to surpass. Unfortunately, it is not constant and varies with air speed and rotational speed, or more precisely with the dimensionless propeller advance ratio $J = v/nd$ where n is the number of blades and d their diameter (Figure 2.18) . As the propeller rotates through one circle the airplane advances a distance v/n. J is then the ratio of this value and the diameter. For airplanes flying in changing conditions, in terms of speed and altitude for example, a variable pitch propeller can be used at the expense of weight.
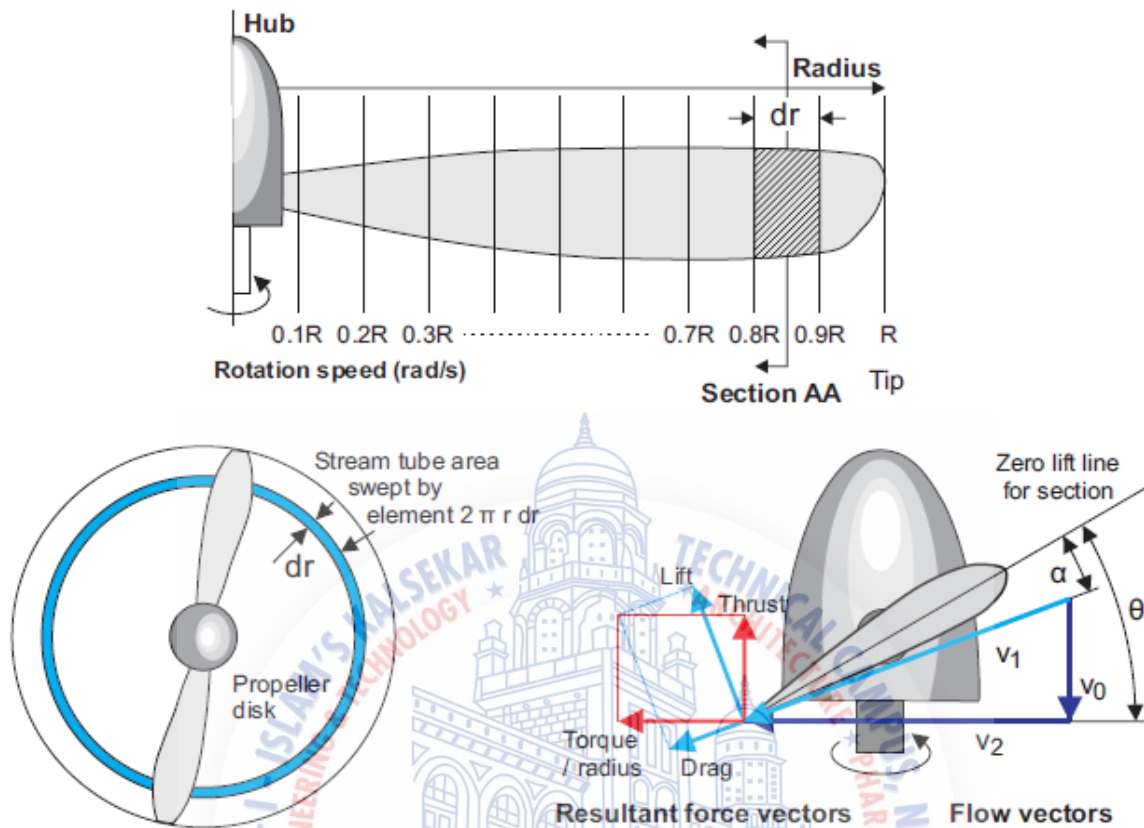
Figure 2.17: Concept of the blade element theory (Source : http://classes.cecs.ucf.edu/eas5157/lin/Ch3-1.ppt)

CHAPTER 3

Chapter 3
Conceptual Design Methodology

3.1 Introduction

This chapter is the theoretical heart of this thesis as it describes in detail the conceptual design methodology. Whether it is intended to achieve surveillance at low altitude or serve as a high altitude communication platform, a solar aircraft capable of continuous flight needs to fly at constant altitude. In fact, the first one would be useless for ground surveillance at high altitude and the second one wouldn't cover a sufficient area at low altitude. For this

reason, we concentrate the following study on straight level flight only, storing the surplus of solar energy in the battery. Other scenarios, such as storing energy through potential energy in altitude or using ascending thermals, will also be treated but later on in chapter 6.

Our methodology is based on two simple balances, which are represented in figure 3.1.

• weight balance : the lift force has to be equal to the weight of all the elements constituting the airplane

• energy balance : the energy that is collected during a day from the solar panels has to be equal to or higher than the electrical energy needed by the airplane.

From here on, and considering the type of mission and the payload to embed, there are two different methods to achieve the airplane conceptual design :
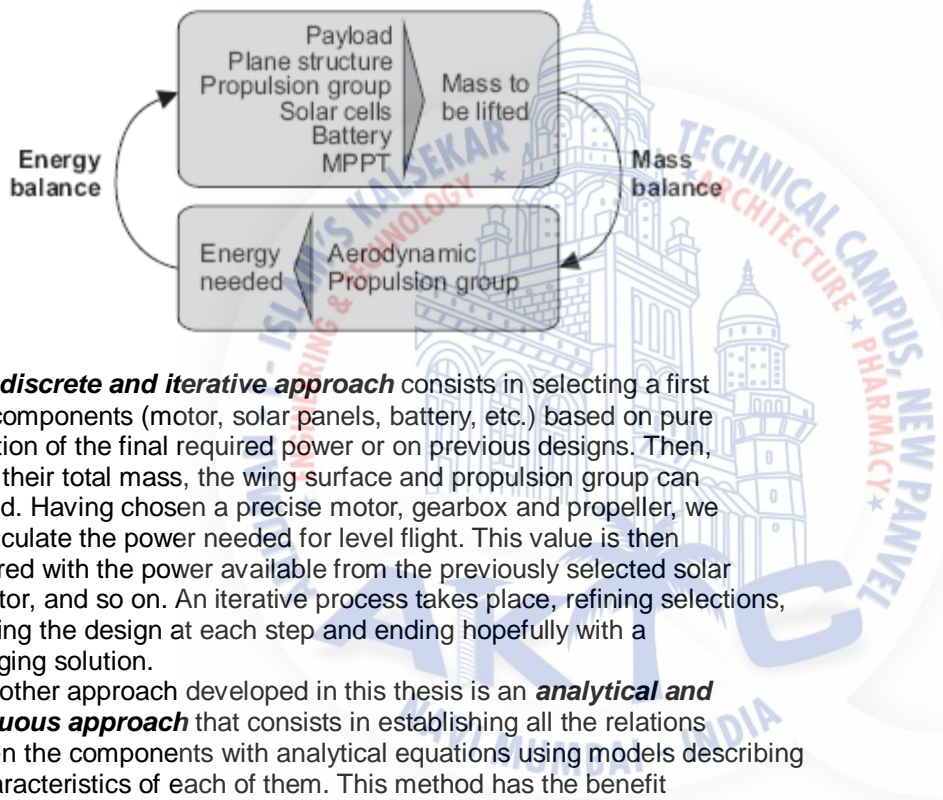
1. The ***discrete and iterative approach*** consists in selecting a first set of components (motor, solar panels, battery, etc.) based on pure estimation of the final required power or on previous designs. Then, having their total mass, the wing surface and propulsion group can be sized. Having chosen a precise motor, gearbox and propeller, we can calculate the power needed for level flight. This value is then compared with the power available from the previously selected solar generator, and so on. An iterative process takes place, refining selections, improving the design at each step and ending hopefully with a converging solution.

2. The other approach developed in this thesis is an ***analytical and continuous approach*** that consists in establishing all the relations between the components with analytical equations using models describing the characteristics of each of them. This method has the benefit of directly providing a unique and optimized design, but requires very good mathematical models. In the present case, an important effort will be made to have these models as accurate as possible on a very wide range, so that the methodology can be applied for solar MAVs as well as for manned solar airplanes.

In the following sections, we will first establish the expression of the power needed for an aircraft at level flight and then present the irradiance model that will lead to the daily solar energy available. After that, we will develop the weight prediction models for all the airplane elements, which will close the loop before presenting the analytical resolution and the solution of the problem.

In order to lighten the equations, substitution variables a_i will be used instead of long formulas. The reader can easily go through the design process keeping an eye on figure 3.17 that summarizes in a very simple graphical way all the calculations and models hereafter.

3.3.2 Calculation of the Daily Solar Energy

The total electric energy is obtained by multiplying the result of equation (3.8) with the surface of solar cells, their efficiency and the efficiency of the MPPT. Additionally, we have to take into account the fact that the cells are not disposed on a horizontal surface but follow the cambered airfoil. In a series of interconnected cells, the one with the lowest irradiance limits the current for all the others. This problem occurs mainly at sunrise or sunset, when the sun elevation is low, and depends also on the airplane orientation. This situation is represented in figure 3.4 where the first cell, near the border of attack, has the smallest elevation angle $\_1$ and will then penalize the other cells.

Figure 3.4: Variation of incidence angle on the solar cells for a cambered wing at sunrise or sunset

For this reason it is important to take care about the wiring configuration and preferably dispose the cells connected in series along the wing, so that they have the same orientation. Simulations have been realized in order to study this impact and the results show that compared to a flat disposition, the camber decreases the energy by almost 10% during a whole day in central Europe. In order to take this effect into account in our methodology, we will consider a new efficiency $\_{cbr}$ that is above 90 %. Thus, the daily electrical energy is :

$$E_{elec\ tot} = \frac{I_{\max}\ T_{day}}{\pi/2} A_{sc}\ \eta_{wthr}\ \eta_{sc}\ \eta_{cbr}\ \eta_{mppt}$$

3.4 Mass Prediction Models

For each part on the airplane, a good mass model is necessary in order to calculate the total mass m and use it in equation (3.5). In this section, we will go through all the parts constituting the airplane and establish their mass models.

3.4.1 Fixed Masses

First of all, there are some fixed masses that will not depend on the sizing of other parts. In this category, we include the payload that is a mission requirement defined at the beginning. To some extent, we can also include the autopilot system if defined at the beginning also. **3.4.2 Airplane Structure**

The mass of the airplane structure is certainly the most difficult part to model and the two main approaches widely used in the literature for solar airplanes appeared inadequate at a scale of a couple of meters. That is the reason why we will study this part more in details and propose a new model valid for sizes on three orders of magnitude.

The first approach from D.W. Hall [69] consists in calculating separately the mass of all the elements constituting the airframe, i.e. the spar, the leading and trailing edges, covering, ribs, control surfaces, fuselage and tail as functions of the total mass, aspect ratio and wing area. The method is very detailed and precise. However, their authors clearly limit its validity for airplanes with a weight between 1000 to 3000 lbs, which corresponds to a mass of 453 to 1360 kg. It was applied by Colozza [50] on a solar airplane

with more than 60m wingspan but is inapplicable in the range of UAVs or MAVs. The second approach, proposed by W. Stender in 1969 [120], is based on statistical data for sailplanes with twin boom tails. The entire airframe weight W_{af} is estimated in a parametrical way as a function of wingspan b, surface S and number of boom tails n, A and B being constants.

$W_{af} = A\, n\, S\, b_{3\_B}$ (3.11)

Data and calculated estimates of airframe weight, ultimate loads, and airplane geometry of MacCready's Solar Challenger and another high-altitude solar powered airplane design concept were used in a regression analysis to define $A = 0.310$ and $B = 0.311$ (Imperial Units lbs/ft) for a class of ultralight, cantilever wing airplanes with twin boom tails [131]. Once converted in the Standard International Unit System (Metric Units), and using the aspect ratio definition $AR = b_2/S$, we can rewrite :

$$W_{af} = 8.763\, n^{0.311}\, S^{0.778}\, AR^{0.467}$$

This model was widely adopted by Bailey [27], Colozza [49], Irving [70], Romeo [113], Youngblood [131] and also Rizzo [110] who additionally proposed his own model obtained by interpolating NASA prototypes data and that is said to be preferred for UAVs.

$$W_{af} = 15.19\, S^{0.656}\, AR^{0.651}$$

Another model used is to consider the airframe weight proportional to its surface. Guglieri makes this same assumption using 2.5 kg/m2 [66, p.50] for a manned version, as well as Brandt who considers a ratio of 0.97 kg/m2 [36, p.706] for his 61m HALE. For their 38 cm solar powered MAV "SunBeam", Roberts et al. [111] used a value of 0.2 kg/m2. Rehmet [105, p.5] considers the formula $M_{af} = 0.103\, [kg/m2]\, b_2 + 1.157\, [kg/m2]\, S$ which can be rewritten as $M_{af} = (0.103/AR + 1.157)\, S$ leading here again to a linear model between airframe mass and wing surface.

Validation of the Model

In order to verify these models, a database containing the parameters of 415 sailplanes of various dimensions was created. They are divided into 92 radio-controlled unmanned models and 323 manned sailplanes. For each of them, the following values are available : wingspan, wing area, aspect ratio, structure weight and gross weight. Figure 3.5 presents the structure weight of these 415 sailplanes with respect to the wing area, the color representing the aspect ratio. On both axes, a logarithmic scale is used to have good global view of the tendency, from the radio-controlled models in the lower-left corner to the manned sailplanes in the upper-right part.

The objective now is to see if the equations mentioned above, which are extensively used in solar airplane designs, follow this tendency. For this purpose, the Stender and the Rizzo models are plotted on the same graph, using two different aspect ratios of 15 and 30. The result is that Rizzo's equation approaches the best sailplane models, which is normal as it was derivated from unmanned solar airplanes data, but it is not convenient for small scale models where it is too pessimistic. In fact, for an airplane with 0.3m2 wing area, it would predict a weight 10 times bigger than in reality.

Concerning Stender's equation, we can see that it is far too optimistic for manned airplanes and also too pessimistic for small scale models.

Chapter 4
Sky-Sailor Design

4.1 Introduction

The methodology that was presented in the last chapter will now be put into
application, with the concrete example of the design of the Sky-Sailor prototype.
After the presentation of the airplane layout resulting from the design
methodology in the next section, we will present a second tool to validate
the concept before building a first prototype. It consists of a simulation environment
that allows analyzing the energy flows on the airplane, between the
solar panels, the battery and the power consuming elements second after second
during a flight. This step is closer to the real experiments and constitutes
an additional proof that the planned airplane will reach its objectives.
The goal of the Sky-Sailor project is to design and build an airplane
that proves the feasibility of continuous flight, over 24 hours, as explained in
section 1.1. This flight should be feasible within 3 months in summer, which
sets the day duration to 13.2 hours according to figure 3.3. A 50 g payload
consuming 0.5 W, representing a small camera and its transmitter, will be
installed onboard. The airplane will fly at a low altitude of 500m above
sea level, 100m above ground. These mission parameters are summarized in
table 3.6 and the technological parameters in table 3.5.

4.2 Application of the Design Methodology

We will now investigate, with the mission and technical parameters that we
considered, what would be the layout of an airplane capable of 24 h flight in
these conditions. For this purpose, various airplane wingspans and aspectratios are tried methodically. For each
combination, equation (3.38) determines
if the solution is feasible. In the case of a positive answer, equation
(3.35) is solved to find the airplane gross mass.
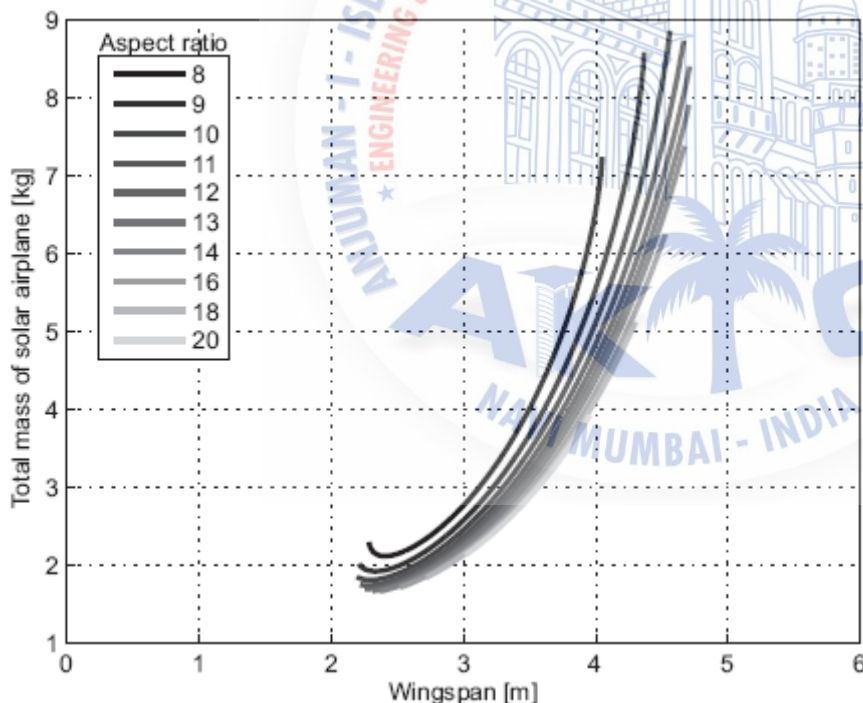
Figure 4.1: Possible configurations presenting the total mass as a function of the
wingspan b and aspect ratio AR

Figure 4.1 presents the results. We can observe that the minimum wingspan
the airplane should have for continuous flight is 2.5 m. There is also an upper
limit, showing that with a wingspan greater than around 4.5m continuous
flight is no longer feasible. This might be surprising, but it has a very simple
reason : with the weight prediction model that we considered, the airframe
becomes too heavy above a certain wingspan so that it is no more possible

to fly continuously with the available power. That means that going higher in dimension would require a lighter airframe weight model. This point will be further discussed below, with the help of figure 4.4.

Having found the total mass for each possibility, we can then introduce it into the loop represented in figure 3.17 to calculate precisely all the other airplane characteristics : powers at propeller, gearbox, motor and battery, surface of wing and solar panels, weights of the different subparts and also flying speed.
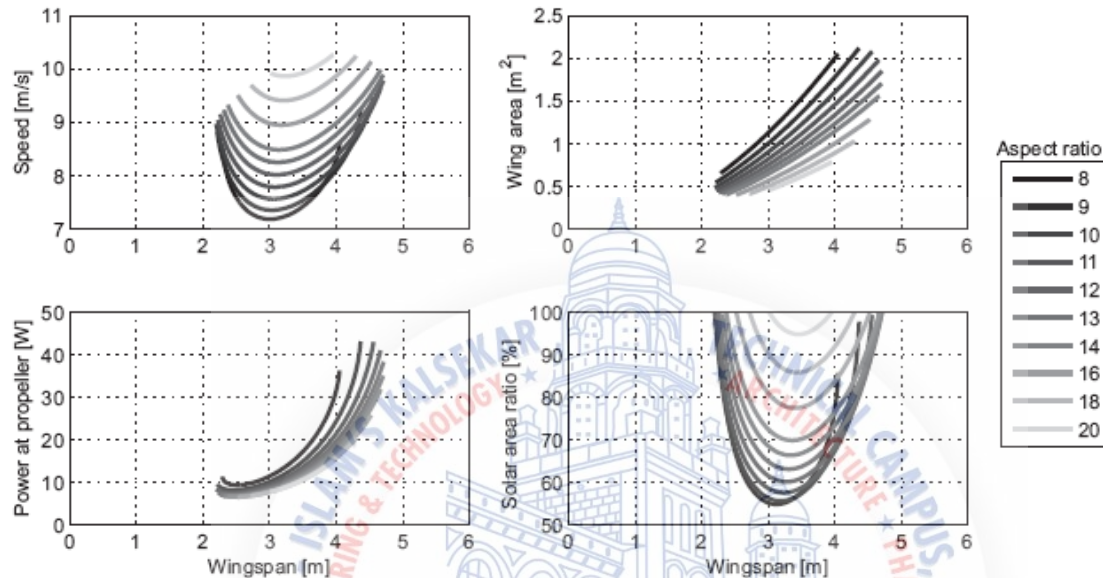
Figure 4.2:

Aircraft and flight characteristics depending on the wingspan *b* and the aspect ratio *AR*

Figure 4.2 presents these data that are decisive for the final selection of the airplane layout. This selection will follow criteria that are determined by the application. They can concern speed, having a certain distance to cover in a limited time, or wingspan, the UAV being stowed in a limited volume and launched by hand. Thus, with the help of these plots, a final configuration can be selected. In the case of Sky-Sailor, one key objective was to study the stowage of the airplane in a very limited cylinder, what would be the case of a system sent to Mars.

Finally, a wingspan of 1.7m including the winglets is considered with an aspect ratio of 11, giving a chord of 19 cm. The targeted airplane weighs 1.5kg, the 60Wh battery and the fuselage representing 40 %, respectively 34% of this amount, as the mass distribution in figure 4.4 tells us. This plot is very useful to see what percentage of the total weight each element represents, in order to orient the research efforts accordingly. One notable point is the airframe weight that sees its percentage increase from 17% to 39% when increasing the wingspan from 2.3 to 4.7m. As the model is roughly cubic, this percentage grows and above a certain wingspan, continuous flight is no more ensured without using a lighter construction technique. Coming back to the selected layout, the mechanical power required for level flight is only 9.42 W, but considering the efficiencies of the propulsion group elements an electrical power of 14.2W will be needed. When adding the autopilot and payload power consumption, the total electrical power is 17.22 W. Level flight should take place at a nominal speed of 8.3 m/s. The wing surface is 0.787m2, from which 0.525m2 are covered by solar cells giving a maximum power of 74W at the output of the MPPT.

Instead of varying only *b*, *m* and *AR*, it is also possible to fix one of

these three variables and use a parameter that was considered as constant as a new variable. For example, we can fix the aspect ratio and then see the impact of air density on the flight feasibility in order to calculate the maximal altitude for a 24 h flight, keeping the same mission objectives. In fact, a potential future step in the project is to fly higher than a few hundreds of meters above the ground. The battery technology being the one that will see improvements the most rapidly in the next years, it is interesting to see the evolution of this altitude with respect to the gravimetric energy density values. This is represented in figure 4.5 that confirms the 3.2m wingspan as a good optimum.

Thus, with this approach it is possible to do far more than just designing an airplane, as a multi-disciplinary optimization (MDO) program would do it. We can easily analyze the impact of some of the design parameters on other parameters or variables. This kind of sensitivity analysis is very useful to observe into which technological domain it is interesting to put efforts in order to increase a certain capability, for example the flight duration. The design methodology that led to the plots here above was implemented under Matlab ℝ. The code is simple and composed of 210 lines divided in four m-files available in the appendix so that the reader can test the methodology himself. In fact, in our design methodology, the added value is not only the program itself but mainly the good models that the methodology is based on. The equations relating them are themselves very simple.

4.3 Real-Time Simulation Environment

In the methodology and its application example presented above, the irradiance is averaged over the whole day, so what comes out at the end is a solution that makes solar flight feasible during this day. However, we might also want to see the flight evolution second per second with an irradiance that varies during the entire day instead of being averaged. It is then possible to monitor all state variables and analyze the energy flows on the airplane from dusk till dawn and from dawn till dusk. This allows validating the design a second time before building the real prototype, but it has other purposes. Such solar flight simulation can predict the charge status of the battery in order to see what the energy margin in the morning will be. This information is very useful then during the real experiments to control for example in the middle of the night if the voltage profile is close to the prediction or not, in which case special measures have to be taken. A second purpose is to see the influence which the alteration of some parameters has on the continuous solar flight. For example, by reducing the efficiency or the area of solar panels, we can simulate dust deposition or damages and evaluate the impact on the feasibility of 24 hours flight. Also, instead of considering only level flight, we are able to test various types of flight at different moments in the day. One example is to start climbing at the end of the afternoon, once the battery is fully charged. Thus the surplus of energy is stored into potential energy. After dusk, when the sun power is not sufficient to power the level flight anymore, a descent to the nominal altitude with the motor off is engaged. Hence, this new tool is definitely not redundant to the design methodology, it is rather complementary.

4.3.2 Simulation of a 48 Hours Flight

The simulation of a 48 hours flight on the 21_{st} of June and starting at 7h00 in the morning is presented in figure 4.7. This day has theoretically the shortest night duration and is thus the optimal period to fly continuously. The left part concerns the power transfers. Considering only level flight, the total power consumption in green is constant, but of course the electrical power coming from the solar panels augments until a maximum of 72W at around noon. During this period, the battery is charged with the power surplus. At

12h10, the battery is charged and during the afternoon, only a power equal
to the power consumption is acquired from the solar panels. This is similar
to what happens in the reality, meaning that having a full battery, it is not
necessary to dissipate the power surplus through a heating resistor becauseso that only the consumed power is
retrieved. At 18h, the solar power is
not sufficient anymore and the battery starts to be used, with a phase where
both the solar panels and the battery are supplying power. During night, the
supply comes from the battery only.
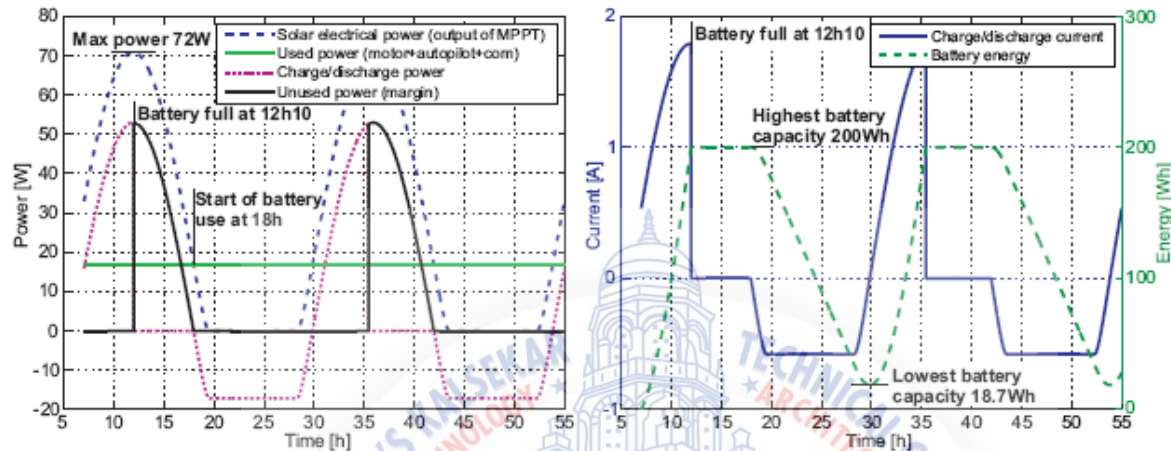
Figure 4.7: Continuous flight simulation

Thus, the bold curve shows that almost half of the energy is not used. The
reason is that this graph shows ideal sun conditions, whereas in reality some
clouds can obstruct the sky during some periods and thus lowers the available
solar power. In this case, the battery would be fully charged later than the
prediction, or if the solar power is really lower than the power consumption,
the battery would even be discharged during the day. If this last situation
occurs during a short time in the middle of the afternoon, it is not so critical
as the battery can be fully charged again before dusk arrives. This is precisely
why in our design a margin factor _wthr was considered (Equation 3.8). If it
happens precisely at dusk or at down, this becomes more problematic because
the battery will start, or respectively end its nocturnal discharge before the
planned hour, what could prevent achieving a new 24 h cycle. In the present
case, the right part of figure 4.7 shows that we have a battery capacity margin
of 18.7 Wh, what represents more than one hour of flight.
In order to be consistent, we should also mention that an ideal battery
model was considered. In reality, the power charging the battery has to be
limited during the second charge phase with constant voltage and decreasing
current (Figure 2.12). Hence, the charging time is slightly lengthened compared
to the case where the battery is constantly charged at 1C (see section
2.4.1).
Now we can do the same simulation but one and a half month later,
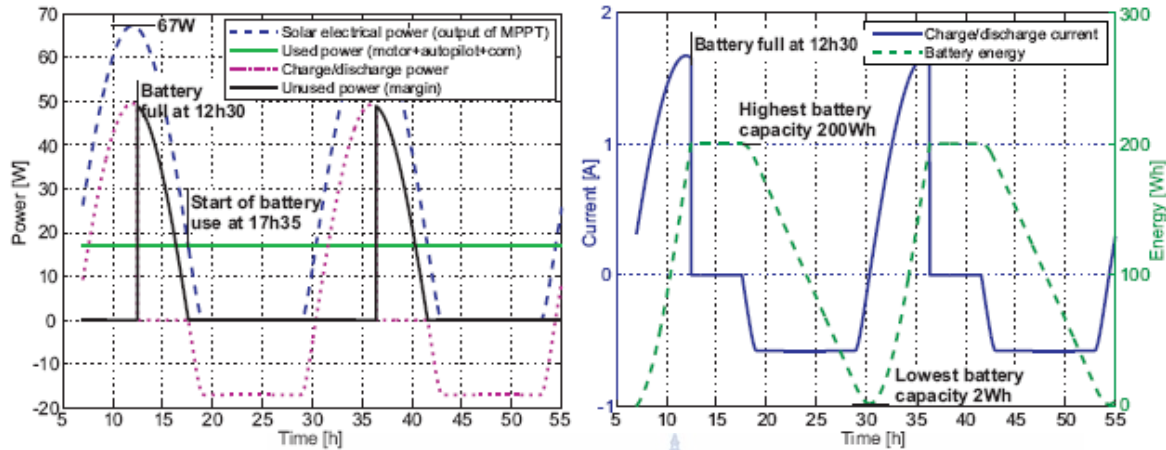
Continuous flight simulation on the 4th of August
as we considered a feasibility margin of three months in summer. Figure
4.8 presents the case with the same airplane and also starting at 7h00 in
the morning, but on the 4th of August. The maximum solar power already
decreased by 7% but this is not critical as a certain margin was considered.
It results only in a battery that needs slightly more time to be charged. The
problem comes from the night which lasts longer now. As a consequence,
the battery starts its discharge 25 minutes earlier than on the 21st of June,
leading to a minimum capacity of only 2Wh at the end of the night.
After this date, the feasibility is no more ensured. That shows clearly
that for achieving continuous solar flight far away from the 21st of June,
what becomes problematic is not the day duration that decreases but mostly
the night duration that increases. And the reason lies simply in the fact that
even with the best energy storage technology available now, the battery is
still very heavy, constituting around 40% of the airplane's weight.

Chapter 5
Mini impulse Realization and Testing

5.1 Introduction

After the presentation of the conceptual design in the last chapter, this section
addresses the preliminary and detailed design of the Sky-Sailor solar airplane.
In fact, whereas so far only the sizes and masses of the airplane elements were
determined using the weight prediction models, the target is now to choose
the exact parts that will be assembled to build the prototype.
This chapter will thus be very practical, presenting not only the selection
of each component but also discussing the possibilities that were offered and
then the criteria and the approach that led to each final choice. In order
to validate the theory, we will then also compare the real characteristics
obtained with the theoretical predictions. The last part of the chapter will
present the flight experiments that were conducted with the fully functional
prototype and compare them with the capabilities that were predicted.

5.2 General Configuration and Structure

According to the results of the design study using the methodology presented
before, a fully functional prototype was built with the name Sky-Sailor.

The general configuration of the airplane is a 3 axis motorized glider,
meaning that the control surfaces are the ailerons, the elevator and the rudder.
Figure 5.1 presents the drawings and dimensions of the airplane that has
a dihedral wing and a V-tail. The aerodynamic design and construction of the structure was achieved by Walter
Engel, a world expert in ultra-lightweight
high performance model sailplanes. The basis layout was adapted from his
Avance glider that set two world records in distance (424.5 km) and duration
(15 h 12m30 s) in the F5P category of FAI in 1998 . The empty
airframe, including the control surfaces and their actuators, weighs 0.725 kg,
for a wingspan of 1.6m and a wing area of 0.776m2. It is thus slightly better
than the 5% model developed for the design phase that predicted
0.870 kg.

Figure 5.1: Drawings and dimensions of the mini impulse prototype

The wing structure is essentially made of balsa wood. A main spar carries the bending and torsion
loads along the wing, and wing ribs, disposed in the direction of flight but
also in diagonal to improve resistance to torsion, give the aerodynamic shape
to the wing. The while the upper side is directly closed by the solar panels that are glued on
the spar and the ribs, and follow exactly the airfoil shape thanks to their
flexibility. The wing is in fact composed of three parts (left, central and
right) that are connected mechanically using dihedral braces. On the two
sides of each of these parts, where they are connected to each others, a zone
of 2 cm width was not covered with solar panels for two reasons. First, high
torques and forces are transmitted between the parts, which could break a
solar cells placed too close to this junction. Second, for the flight experiments
a very resistive duct tape is applied on this zone to add security at thejunction between the two parts. Figure 5.2
presents the right and the middle
part of the wing, with and without solar panels so that the reader can observe
the ribs architecture.

5.3 Airfoil

In the design process of an airplane, the airfoil selection is very important and
always different because of the various applications, flight speeds, etc. In the
present case, the selection criteria are first the ratio $C_D/C_L^{3/2}$ that is part of
equation (3.5) for the calculation of the level flight power. The airfoil should
also be especially good at low speed because of the low Reynolds number. At
level flight, Sky-Sailor will have a speed of 8.3m/s what leads to a Reynolds
number of around 150 000 using equation (2.3).
There are many programs to calculate the lift, drag and moment coefficients
of a wing section. In addition to the complex Computed Fluid Dynamics
(CFD) programs that use finite elements methods, there are several
other programs that are limited to 2D calculations. We can mention X-foil,
Javafoil, Winprof among many others. The mathematical models that they
use to calculate the pressure distribution vary and as consequence, they are
all efficient for a specific flight domain. Some will give good results for the selection
of an heavy high speed aircraft profile, some others are more suitable
for lightweight slow gliders. For this reason, we shouldn't be astonished to
see different results coming out of two programs while the profiles and flightconditions entered are similar. It is just
important to take their domain of
validity into account.
Whereas the airfoil used for the V-tail is a standard symmetrical profile
NACA0008, the one used for the wing was specifically designed by W.
Engel for that precise application and named WE3.55-9.3 (Coordinates in
appendix C). The lift and drag coefficients are plotted in figure 5.5 for different
Reynolds number using the program X-foil. For angles of attack between
-2 _ and 8 _, the airflow around the profile is laminar what gives valid data.

Outside this domain, one can observe that the drag increases rapidly due to the fact that an airflow separation occurs leading to turbulent zones, as explained in section 2.2. The behavior then becomes very difficult to predict and even if the software outputs data, it should be considered very carefully. In fact, only real experiments in a wind tunnel can correctly predict what happens then.
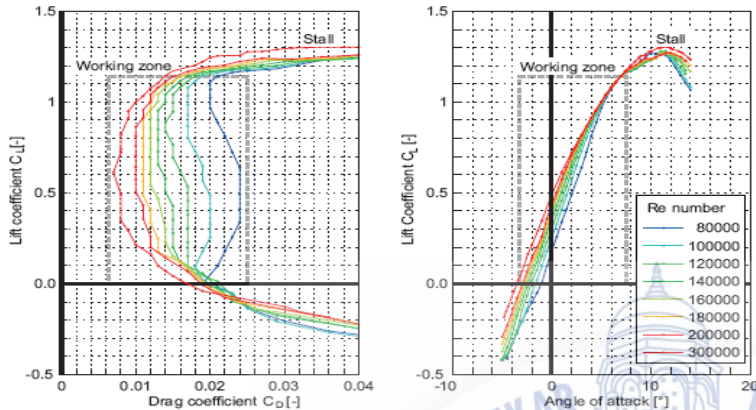
Figure 5.5: Polars of the WE3.55-9.3 airfoil using X-foil

The angle of attack used in the case of Sky-Sailor for nominal flight will be such that it gives a lift coefficient $C_L = 0.8$ and a drag coefficient $C_{Dafl} = 0.0122$. Then considering the induced drag $C_{Dind} = 0.0152$ and a parasitic drag $C_{Dpar} = 0.0065$ calculated with the Winprof program, we end with a total drag of $C_D = 0.034$ what leads to a glide ratio of 23.5 at a speed of 8.3m/s . It would be possible to choose a higher angle of attack that would slightly reduce the power required for level flight, but the speed would then be very close to the stall speed. It is therefore very important to choose an angle of attack that gives a certain margin before stall for the flight in normal

conditions. Of course, in the case of very calm atmospheric conditions, it is possible to increase the angle of attack of the main wing by some tens of degrees using the elevator in order to be at the minimum power point. Equation (3.4) allows plotting the power required for level flight as a function of the airplane's gross mass. This is done in figure 5.6 considering always the same wing surface of 0.776m2 and battery capacity of 196 Wh. This plot is more useful than it may look like at a first glance. In fact, it will facilitate the selection of the various components by showing the relation between a gain in weight, efficiency and autonomy. As an example, we can wonder if it is worth trading a motor controller that offers 94% efficiency for a new one with 97% efficiency but 20 g heavier. This plot and the equations behind help determining if the weight penalty is compensated by the power reduction thanks to the better efficiency.

5.4 Propulsion Group

The choice of the components that compose the propulsion group, i.e. the motor and its controller, the gearbox and the propeller has to be done carefully with the objective to increase the efficiency while keeping the total weight low. The selection first began with the propeller, because their availability is very restrictive.

5.4.1 Propeller

A fixed pitch two carbon blades propeller with a diameter of 60 cm and a weight of 34 g is used. Named Solariane, it has a Goe795 profile and was designed and built by the high efficiency propeller expert, Prof. Dr. Ernst Schöberl, also a pioneer in solar and man-powered airplanes. Variable pitch propellers are more suitable if the flight conditions often change, because

adapting the pitch can ensure the highest efficiency at each speed, which can even be done automatically with an in-flight thrust measurement. However, this solution requires additional mechanics and control, which means more weight. In the case of Sky-Sailor, flying at constant speed except for the launch and the landing, the fixed pitch solution is the best. A spring system retracts the two blades when they are not turning, which is necessary for landing. Once powered again, they open thanks to centrifugal forces.

The propeller data, especially power, efficiency and thrust, with respect to the rotating and forward speed were simulated using the program WinProp v. 3.01 from W. Westphal, Helmut Schenk and Norbert Graubner. This

program bases its calculation on experimental data.

5.4.2 Motor and Gearbox

Having the propeller, a suitable motor has to be found that, combined to a gearbox with the appropriate reduction ratio, maximizes the efficiencies product of the three elements. It was not the goal here to design and build a special motor, but rather to find the most suitable commercially available one. In order to do this, a routine was written in Matlab ʀ that simulates the operation of a motor, a gearbox and a propeller.

A database of more than 2600 motors for which the no load current, speed constant, resistance and weight information were available was created. It contains mainly all the Maxon motors and includes the Motocalc database, very well known among the model-makers and containing all the main modelmaking brushless motors on the market.

Contrary to the motor, the gearbox will not come from the market but will be built specifically. Hence, it is possible to reduce the weight compared to commercial products and choose a very precise and optimal reduction ratio. Gearboxes with reduction ratios from 1 to 20 with a step of 0.1 were considered. The limit is set to 20 because above this value, the efficiency starts to drop below 90% which is not desirable (Figure 3.14).

Then, all the combinations between these motors, gearboxes and the propeller were simulated to find the best trade-off in terms of efficiency and weight. The theory behind this program and the results are shown here after.

5.5 Control Surfaces Actuators

The four control surfaces, i.e. the two ailerons and the two parts of the V-tail, are actuated by what is called in the model-making world "servomotors" and often abbreviated "servos". A servomotor has an axis, the angular position of which can be precisely set in a limited range of less than one turn, generally around 90 _. It is composed of a DC motor, a very high reduction ratio gearbox and electronics that steer the motor based on the angle measured with a potentiometer connected to the main axis.

Many products are available on the market, but generally of very poor quality and without any specifications on their reliability during long periods of use. For these reasons, a test bench was built where many servos were tested with the same torque and angle deviation as on the airplane. The current consumption and the temperature were monitored continuously. The worst servomotors broke or saw their temperature dramatically increase after less than 24 hours. The most common reason was the rapid usury of the potentiometer contact that blocked the axis. However, the best products held 20 days without any problems or significant power consumption increase. This was the case of the S100 from Becker, a 13 g coreless servomotor with metallic gearbox, which was used for the ailerons. For the V-tail, two Dymond D47 weighing 4.7 g with plastic gearbox were used. They showed fatigue after seven days but were still the best in this low weight category. Thus, for a 24 or 48 hours flight commercial products can be used after a careful selection,

but a one week solar flight would for sure require a special development.

5.7.4 Maximum Power Point Tracker

After a survey of the market, no off-the-shelf MPPT seemed to be available, that fitted our application and met our tight requirements. That is the reason why an own MPPT was designed. Five successive versions were built with, at each step, improvements in the direction of dimensions, weight and efficiency.

Hardware

The MPPT is composed of three DC-DC converters with adjustable gain controlled by a microcontroller, put together on a single printed circuit board. Their inputs are connected separately to each of the three solar panels and their output is connected in parallel to the battery (figure 5.16). A good design is necessary to minimize the losses that reduce the efficiency, especially occurring in the inductor (L1) and the conducting diodes (D1-D4) that were put in parallel to minimize the individual currents and thus the dropout voltage [90].

Figure 5.15: Schematic of the solar generator

Figure 5.16: DC/DC converter block of the maximum power point tracker for a single solar panel. The two other blocks and parts like the microcontroller, temperature sensors, MosFet drivers and voltage sensor were omitted here

The high switching frequency of 100 kHz with currents that can go up to 5A in total can cause electromagnetic interferences that disturb the antennas present on the airplane. For this reason, a shielding in a special material named mu-metal covers the board on which the last layer is a ground plane. The shielding itself is also connected to the ground. The last version of the MPPT has a measured efficiency between 95% and 97%, depending on the power that can go up to 100 W. It weighs 25.86 g yielding a power to weight ratio of 3.87 kW/kg . This is higher than the 2.37 kW/kg predicted with the interpolation in figure 3.10.

Figure 5.17: mini impulse high efficiency and lightweight MPPT

5.10 Final Prototype

The above explained sections are the major component of solar plane we can also add the auto pilot system to the plane to navigate the plane through GPS. In our design the 25w 1.7 amp solar cell are used to power battery and the motor for level flight at the day time solar cell supplies power to the motor and Battery which takes 7hrs to full charge the battery at the night time battery supplies power to the motor up to 2.5 hrs to extract maximum power from the solar cell we uses PWM solar charge controller MTS brand which select the most appropriate point of V-I characteristic of solar cell which also provide additional protection to battery at the time of low   and high voltage we also uses high capacity motor to provide high starting torque for takeoff. The total weight of the plane is 1100 gram's with the help of balsa wood .For wing's design Clark y airfoil is used to reduce the drag due to the wings of plane. We also use top wings design structure to increase the roll stability of the plane.

Figure 5.23: The mini impulse prototype held by the author and during a flight

Conclusion

7.1 Main Achievements

This thesis presented a new methodology for the conceptual design of solar airplanes. It has the advantage to be very versatile and usable for a large range of dimension, from UAVs with less than one meter wingspan to manned airplanes. It is purely analytical and based on the concepts of energy and mass balances during one day using mathematical models that put the sizing of all elements on the airplane in relation. These models are used for efficiency or weight prediction and constitute a key part of such design method. They were not only studied in a limited domain, but over a very large range, for some models with up to 7 orders of magnitude, showing for example on the same graphics a tendency that encompasses motors from 1mW to 10 kW. Finally, the design methodology consists of a simple routine that takes 5 parameters linked to the mission and 25 to the technologies used as inputs. It allows the designer to output the layout of a solar airplane rapidly, with size, weight and power informations.

The methodology was used for the conceptual design of a prototype that would embed a small payload and with the objective to prove the feasibility of continuous flight on Earth. It also allowed emphasizing some general principles. For example, it was clearly demonstrated that the most limiting technology at this time is the energy storage. Even with the best lithium-ion batteries, the energy storage constitutes more than 40% of the airplane's gross weight. For that reason, what is critical for a continuous solar flight is not the day that has to be the longest, but the night that has to be the shortest. Name mini impulse, it validated the theoretical part of this thesis through experiments and proved the efficiency of the design methodology by achieving a flight of more than 14 hours using only solar power. This achievement is a record for a UAV that doesn't use altitude gain or thermal updrafts. With the development of this prototype, a considerable amount of practical knowledge and experience was acquired in various fields such as aerodynamics, lightweight structure construction, solar energy management, sensor fusion, efficient electronics, control, etc. For all of the airplane components, tradeoffs were to be made between efficiency, power consumption and weight.

Figure 7.1 presents the losses on the energy train from the solar cells to the propeller and emphasizes the fact that a careful design of each part is necessary. This results in a precious know-how that wouldn't have been acquired if the project had stayed at a simulation level.
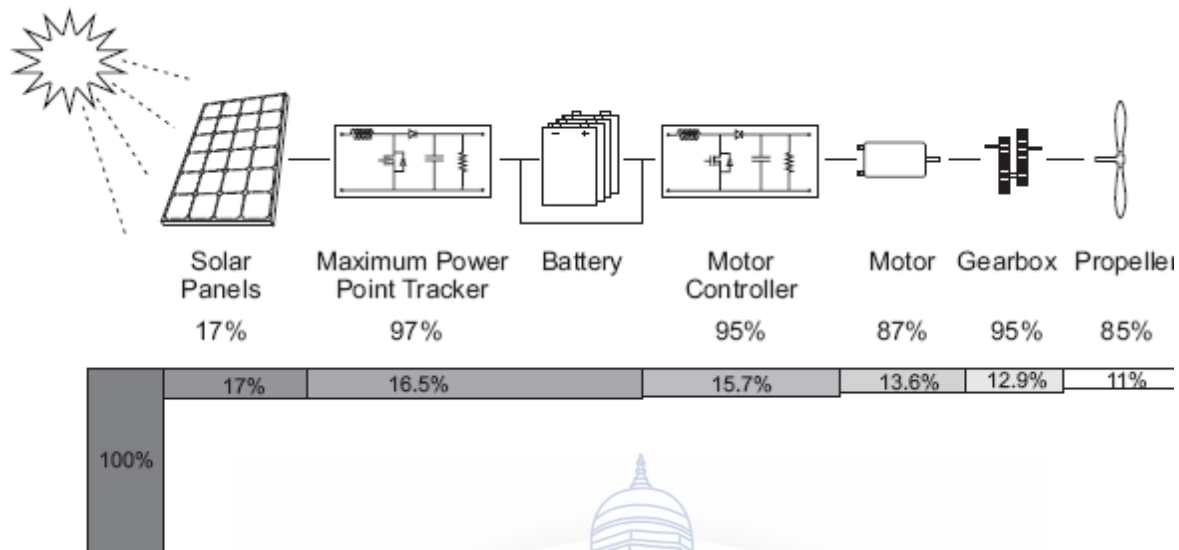
Figure 7.1: Energy train on the mini impulse solar airplane with the cumulated efficiencies
The design methodology being valid over a wide range of dimensions, a
part of this thesis was also dedicated to study the scaling of solar airplanes
and thus to clearly identify what becomes problematic at large or small dimensions.

3. Potential Applications and the Future of Solar Aviation

Without intending to predict the future, the experience gained during this thesis allows us to foresee the direction that solar aviation will take and the applications that it might cover. It is obvious that the technologies involved in the construction of solar powered airplanes will see many improvements these following years, with the growing need of green solutions for transportation, consumer electronics, etc. The first solar powered airplanes used for concrete applications will probably have a size between 3 to 6 m. In fact, it was proved in section 6.3.3 that this range is somehow optimal and allows already now continuous flight with the current technologies. Moreover, applications such as law enforcement, border surveillance, forest fire fighting or power line inspection would require a payload of not much more than 1 kg what is precisely the capacity in such

wingspan range. So for these applications, the next 10 years will certainly see a rapid and important development of solar powered UAVs at the size of some meters.

At the MAV range, improvements will be necessary before seeing a flying robots of the size of a hummingbird, powered by the sun only. The low Reynolds number will always be a limiting factor, but with more efficient

solar cells and propulsion group elements, added to a better energy storage, the dream should once come true. Miniaturization of the electronics and the avionics will also play a major role. embedding a human person or for instance a payload of 150 kg for a perpetual flight imposes a huge wingspan and requires a very lightweight

wing that turns out to be fragile, leading to an airplane that is not easily steerable. One could of course say that with improvements of technology, it will become feasible in some years, as it was not predictable after the Wright brothers' flight that there would once be airliners crossing the Atlantic with 500 passengers onboard. The author thinks that this will never happen, for many combined reasons. The first limitation comes from the sun irradiance that even with 100% efficiency solar cells would never provide enough power to not only carry the passengers, but also a minimum of comfort which implies a lot of additional weight. Linked to this, the cubic tendency of the airframe's weight is not compensated

by the square tendency of the solar cells surface,

. The large surface of solar cells needed leads then to impressive wingspans. Also, we observed that the speed of a solar airplane doesn't exceed 50 km/h making trips last several days instead of hours as with an actual airliner. That lets us believe that solar propulsion has a future for transportation only for trips that don't exceed 24 hours and for one or two persons onboard. Even in this case, a far better solution would still consist in using solar

energy, but in a concentrated form. In fact, one could cover the roof of airports and hangars with solar panels and use this energy to hydrolyze water into hydrogen and oxygen. The hydrogen would then be stored and used on the airplane in a fuel cell. To summarize, what makes solar airplane not so ideal is that they have to embed the whole factory that converts the few energy coming from the sun in real-time, which is, as we saw, a heavy and not so efficient undertaking. Thus, the better idea is to let this heavy factory on the ground, concentrate the energy, and then only use it on a fast airplane with reasonable dimensions and thus a correct manoeuvrability. One part of the wing could still be covered by solar panels, but to cover only a small percentage of the electrical power consumption. For solar HALE platforms anyway, it is different. The reason is that here the objective is not to transport something from A to B in a minimum of time but rather to ensure the presence of a given payload at a certain location and altitude during months or years. In this case, no energy storage method available now is good enough to embed the whole energy needed for the flight as a concentrated form. Thus the collection of solar energy directly onboard the airplane is so far the only solution. Such platforms will certainly be used in some years for telecommunication or Earth monitoring. Nevertheless, the payload they will be able to carry will always be very limited, due to the problems that were mentioned here above.

3.1 Environmental Benefits of Solar Aircraft

Many researchers say it's useful to park a solar aircraft in the sky. It can hover over a spot, carrying cameras or other sensors. In the stratosphere, it can sample gases near the ozone layer. It can also watch forest fires or track hurricanes on the ground.

For the military, solar airplanes can help with reconnaissance. Like spy planes, they fly high, which makes them stealthy. But while spy planes must fly over and return, solar airplanes are unblinking eyes. They can take uninterrupted photos or videos for years. "When an event happens, they can study everything that led up to it," says Del Frate. For law enforcement, they're good for border and port patrol.

It's true satellites can perform some of these tasks. But solar airplanes see more detail on the ground with less expensive cameras because they're closer to the action. They're also less expensive to build and launch. While satellites are hard to move once they're in orbit, solar airplanes are easily moved. It's also easier to bring solar planes down for maintenance.

Solar aircraft, being electric, emit no exhaust. Commercial airplanes do. In 1992, airplanes emitted 0.5 billion tons of CO_2, or 2 percent of human CO_2 emissions [source: IPCC]. Their exhaust contains many substances linked to health and environmental effects, although the U.S. Environmental Protection Agency (EPA) regulates their levels, and health impacts near airports are being studied

[source: EPA, Wachter]. Regardless, solar planes can't become clean passenger planes because they'll probably never have enough power to carry many passengers, says Del Frate.

Stratospheric jets, like the F-22A Raptor and U-2 spy planes, also emit exhaust. While they emit it into the stratosphere, where gases persist longer than in our troposphere below, their contribution to air pollution, ozone depletion and global warming hasn't been measured thoroughly. Solar airplanes that can accelerate and maneuver like these planes are many years off. So at this time, it's not practical to talk about solar planes being environmentally friendly alternatives to other planes. Still, they are clean vehicles for their current applications.

A surprising benefit of solar airplanes, says Del Frate, is that if solar panel manufacturers supplied a dozen solar planes a year with big, high-efficiency panels, the cost of high-efficiency panels for your home would go down.

CHAPTER 4

4.ADVANTAGES AND DISADVANTAGES

4.1Advantages of Solar Powered Drones:

> **Decreased Operational Cost:**

The biggest hurdle in the drone-carried operations is the high operational cost. Operational hours of drones are limited mainly due to time bound fuel availability in the fuel tank. With the help of solar powered batteries, the fuel charges and operational cost can largely be minimized. Imagine the possibilities, a drone flying in the sky without the need of charging and refueling.

> **Increased Operational Hours:**

Fuel powered drones have a well known problem of limited operation hours. The problem is that a drone can only have a limited amount of fuel in a single flight, if a drone is designed to have increased number of flight hours then it must have a fuel tank big enough to last for long hours but this poses a problem to the stability of the system as the whole equilibrium and balance of the plane is disturbed. Solar powered drones wouldn't have such a problem because they can operate for not only days but years. According to the reports, Solara 50 may remain airborne for years.

> **Weather Warnings & Updates:**

Drones can fly well above the average height in contrast to a normal aero plane, this is due to their stable and light weight structure. Solar powered drones are more lightweight than the traditional and operational

military drones as they don't have a heavy engine to keep it running. These drones can easily assist us by tracking hurricanes, bad weather, approaching storms and tsunami warnings.

> **Calamity Assistance:**

Solar powered drones can easily spot the areas which are hard to reach by human after a disaster. Increased flight hours can assist rescue teams in reaching the target areas, survey damage and spot stranded victims

4.1 Disadvantages of Solar Powered Drones:

> **Battery:**

The biggest challenge that we need to overcome is the life of the battery. Smaller batteries mean limited flight hours. During the day light it is not an issue because there is more than enough sunlight to keep the drone moving but what about night? The answer is batteries but the battery storage is major limitation because it means more weight.

> **Weight Issue:**

Weight and battery issue are directly connected, if the scientists opt out for increased battery life then it will definitely increase the weight of the unmanned vehicle. This may disturb the overall weight shifting of the plane or create imbalance among the structure.

CHAPTER5

5. List of Solar Airplanes Flown to Date

The table below lists all the solar powered airplanes that were built and flown, until 2008, and from which it was possible to obtain dimension and weight characteristics. From the 1 gram SolFly to the 600 kg Helios, they are all sorted here according to the year of their maiden flight and also represented graphically in figure 3.8 in a wing loading vs weight plot. The total weight is the airplane empty weight plus the pilot weight, in the case of manned airplane, or the payload. Airplanes that stayed or still are at

the design phase and were never built so far are not included.

Nr.	Name	Year	Designer	Wing span [m]	Mean Chord [m]	Length [m]	Wing Area [m²]	Aspect Ratio [-]	Empty Weight [kg]	Total Weight [kg]
1	Sunrise	1974	R.J. Boucher from Astro Flight, USA	9.75	0.86	4.38	8.36	11.4	12.25	
2	Sunrise II	1975	R.J. Boucher from Astro Flight, USA	9.75	0.86	4.38	8.36	11.4	10.21	
3	Solaris	1976	Fred Militky, Germany	2.06	0.20		0.41	10.3	0.61	
4	Ra	1977	Prof. Dr. V. Kupciks	1.37	0.12	0.84	0.16	11.9	0.19	
5	Utopie	1977	Dr. Roland Stuck, France	2.53	0.20	1.32	0.51	12.6	0.97	
6	Solar-Student	1978	Prof. Dr. V. Kupciks	1.96	0.22	1.04	0.43	8.91	0.93	
7	Solar One	1978	David Williams and Fred To	20.72	1.17	6.70	24.15	17.8	104.32	
8	Solar-X4	1979	H. Schenk	2.50	0.17	1.13	0.42	14.8	0.85	
9	Solar Silberfuchs	1979	Günter Rochelt	4.00	0.25	1.52	1.00	16.0	2.10	
10	Solar Riser*	1979	Larry Mauro	9.14	1.04	2.44	9.52	8.8	55.80	124.7
11	Solar-HB79	1980	Helmut Bruss	2.80	0.24	1.45	0.67	11.7	1.51	
12	Solair I*	1980	Günter Rochelt	16.00	1.38	5.40	22.00	14.0	120.00	200.0
13	Gossamer Penguin*	1980	Dr. Paul B. MacCready from Aerovironment	21.64	2.63		57.00	8.2	30.84	67.7
14	Solar-HB80	1981	Helmut Bruss	2.84	0.23	1.48	0.65	12.5	1.72	
15	Solar Challenger*	1981	Dr. Paul B. MacCready from Aerovironment	14.80	1.48	9.22	21.83	9.0	99.79	153.0
16	Solus Solar	1984	Helmut Bruss, F.W. Biesterfeld	3.20	0.29	0.88	0.93	11.0	2.20	
17	Poly	1986	Helmut Bruss	3.24	0.29	0.88	0.97	10.8	2.48	
18	Combi	1987	Peter Hartwig	2.96	0.26	0.85	0.77	11.4	2.29	
19	Solariane	1987	Franz Weissgerber, Ernst Schöberl	3.08	0.28	1.72	0.85	11.2	1.80	
20	Helios (model)	1989	Erich Töpfer	2.14	0.18		0.39	11.8	1.40	
21	Bloch	1989	Edwin Bloch	2.90	0.24		0.70	12.0	1.25	
22	Grosholz	1989	Rainer Grosholz	3.07	0.19		0.60	15.8	1.85	
23	Combi 2	1989	Helmut Bruss	2.95	0.28	1.54	0.77	11.3	1.70	
24	Ikaros	1989	Franz Weissgerber	2.50	0.23		0.58	10.8	1.80	
25	Bleher	1989	Wolfgang Bleher	2.00	0.24		0.49	8.18	1.37	
26	Romarino	1989	Urs Schaller	2.00	0.20		0.40	10.0	1.80	
27	Sol-e-moi	1989	Alfred Hitzler	3.00	0.17		0.50	18.0	2.10	
28	Wolf	1989	Josef Wolf	3.00	0.21		0.63	14.3	1.60	
29	WS-Solar	1989	Werner Schleidt	2.50	0.22		0.55	11.3	1.55	
30	Ariane Ultra	1989	Franz Weissgerber	1.98	0.21	1.14	0.41	11.0	3.02	
31	Solar Voyager	1990	Volker Klein	3.20	0.25		0.79	13.0	1.30	
32	Mardini	1990	Hans-Jakob Sommerauer	2.40	0.25		0.60	9.6	2.50	
33	Sollisolar	1990	Edwin Bloch	2.98	0.23		0.69	12.9	1.23	
34	PB 26-FL	1990	Marco Buholzer	2.60	0.22		0.58	11.8	2.30	
35	Solarbaby	1990	Werner Deitweiler	1.70	0.16		0.28	10.4	1.25	
36	Bleher	1990	Wolfgang Bleher	2.00	0.22		0.44	9.03	1.55	
37	Uccello	1990	Josef Kapfer	2.70	0.23		0.63	11.5	1.90	
38	Sole Florentino	1990	Franz Weissgerber	2.50	0.17		0.43	14.6	1.20	
39	Soli	1990	Ernst Schöberl	2.05	0.18		0.38	11.5	1.50	
40	Playboy	1990	Thomas Blay	2.40	0.19		0.45	12.8	1.35	
41	WS12 (then WS16)	1990	Dr. Wolfgang Schaeper	2.50	0.16	1.10	0.41	15.2	0.84	
42	Solar Flyer	1990	Peter Hartwig	2.64	0.23	1.48	0.61	11.5	1.60	
43	Blue Chip	1990	Hans W. Müller	2.20	0.23	1.25	0.50	9.66	0.75	
44	Solarmax	1990	Erich Töpfer	3.48	0.30	1.59	1.04	11.6	2.54	
45	Sollisolar 89-2	1990	Edwin Bloch	2.98	0.23	1.34	0.68	13.1	1.24	

* Denotes manned solar airplanes

BIBLIOGRAPHY

- DARPA. "Vulture Program: Broad Agency Announcement (BAA) Solicitation 07-51." July 31, 2007. (6/4/2009) http://www.arpa.mil/TTO/solicit/BAA07-51/VULTURE_BAA_FINAL.pdf

- Del Frate, John. Personal interview. Conducted 6/4/2009.

- Boeing. "Boeing 747-400: Specifications." 2009. (6/4/2009) http://www.boeing.com/commercial/747family/pf/pf_400_prod.html

- Boeing. "Commercial Airplanes: Jet Prices." 2009. (6/4/2009) http://www.boeing.com/commercial/prices/

- Bush, Steven. "Inside QinetiQ's Zephyr Solar Powered Plane." September 28, 2007. (6/4/2009) http://www.electronicsweekly.com/Articles/2007/09/28/42280/inside-qinetiqs-zephyr-solar-powered-plane.htm

- Environmental Protection Agency. "Regulatory Announcement: New Emission Standards for New Commercial Aircraft Engines." March 17, 2009. (6/4/2009) http://www.epa.gov/otaq/regs/nonroad/aviation/420f05015.htm#pagetop
- Intergovernmental Panel on Climate Change. "What are the Current and Future Impacts of Subsonic Aviation on Radiative Forcing and UV Radiation?" IPCC Special Report on Aviation and the Global Atmosphere. 1999. (6/14/2009) http://www.ipcc.ch/ipccreports/sres/aviation/006.htm#spmfig2a
- Lockheed Martin. "F-22 Raptor." 2009. (6/4/2009) http://www.lockheedmartin.com/products/f22/f-22-specifications.html
- Lockheed Martin. "F-22A Raptor Flight Demonstration."
- NASA. "Helios Prototype." 2001. (6/4/2009) http://www.nasa.gov/centers/dryden/news/FactSheets/FS-068-DFRC.html
- Noll, Thomas et al. "Investigation of the Helios Prototype Aircraft Mishap." January 2004. (6/4/2009) www.nasa.gov/pdf/64317main_helios.pdf
- "Solar Impulse." 2009. (6/4/2009) http://www.solarimpulse.com/
- QinetiQ. "QinetiQ's Zephyr UAV Flies for Three and a Half Days to Set Unofficial World Record for Longest Duration Unmanned Flight." August 24, 2008. (6/14/2009) http://www.qinetiq.com/home/newsroom/news_releases_homepage/2008/3rd_quarter/qinetiq_s_zephyr_uav.html
- United Solar Ovonic. "Solar Laminates." 2008. (6/4/2009) http://www.uni-solar.com/interior.asp?id=102
- Wachter, Sarah. "Airports struggle to reduce their pollution." The New York Times. June 4, 2008. (6/4/2009) http://www.nytimes.com/2008/06/04/business/worldbusiness/04iht-rbogair.4.13465825.html?_r=2&scp=9&sq=airport%20pollution&st=cse